10-1-1974

Thermonuclear Astrophysics

Donald D. Clayton
Clemson University, claydonald@gmail.com

Stanford E. Woosley
Rice University

Thermonuclear astrophysics*

Donald D. Clayton and Stanford E. Woosley†

Department of Space Physics and Astronomy, Rice University, Houston, Texas 77001

We discuss the types of thermonuclear reactions that are of importance to stellar evolution and nucleosynthesis, with particular attention to the explosive ejection of shells of He, C, O, and Si. We present tables of the reactions important in the various burning phases, including the reason for their importance and an estimate of the value of a carefully measured rate. This format is chosen for dual purpose: (1) to clarify the nuclear needs by evaluating the importance of specific reactions within the astronomical settings and (2) by assigning a value scale for cross-section measurements.

I. INTRODUCTION

Nuclear astrophysics includes many things: the structure and evolution of stars, the synthesis of the elements in stars, the nuclear debris from the beginning of the universe, the structure and formation of neutron stars, pulsars, and black holes, the origins of cosmic rays and their interactions with interstellar gas, the chemical evolution of galaxies, the history of the planets and the moon, solar-neutrino astronomy, and nuclear gamma-ray line astronomy—to name those that come quickly to mind. In a sense, nuclear astrophysics involves most of astrophysics, because there are few important events in astronomy, cosmogony, and cosmology that have not left nuclear clues. We may gather these clues, study the properties of the atomic nuclei, and, if we are lucky, figure out what has happened.

In this paper we want to narrow our view to consider the thermonuclear reactions that occur during the evolution of stars, and even more specifically, during the thermonuclear explosions of carbon, oxygen, and silicon that have apparently synthesized the abundant nuclei between elements neon ($Z = 10$) and nickel ($Z = 28$). These thermonuclear explosions have outlined new vistas for laboratory nuclear astrophysics. Many more reactions now have importance than was formerly thought, and, at the high temperatures of these explosions, most of them can be directly measured in the energy range of interest. The main purpose of this paper is to provide tables of the nuclear reactions important during these burning phases, to tell why each reaction is important, and to indicate how valuable a measurement of the actual value of the cross section will be to astrophysics. This is an ambitious effort, and in such a rapidly advancing field we cheerfully acknowledge in advance that some oversights and mistakes will be made. Nonetheless, we hope the effort will be useful for both nuclear physics and astronomy.

In doing this we have placed heavy reliance on our own work, which constitutes most of the references. The reference lists of those papers, however, can provide a much more thorough bibliography. We are not attempting a bibliographic review here, but instead hope to stimulate research with this new survey of thermonuclear astrophysics. We also have not attempted to cover all of the interesting subjects in thermonuclear astrophysics, preferring instead to give thorough coverage to the specific burning phases and processes that we tabulate. For these, at least, we also provide a modern sequel to the now classic review by Burbidge *et al.* (1957), which appeared in this journal seventeen years ago.

II. THERMONUCLEAR REACTIONS: LABORATORY PROBLEMS

Laboratory nuclear astrophysics has often been a frustrating science. The desired cross sections are among the smallest measured in the nuclear laboratory, and often require long integration times with painstaking attention to background. The small cross sections are due to the supression of particle widths by the Coulomb barrier, of course; however, many of the reactions now of interest are not so inhibited as were the classic ones. From a purely nuclear point of view, moreover, the reactions studied are often of comparatively little interest. It is their application to astrophysics that provides the major intellectual motivation. However, experience has revealed many occasions when the evaluation of thermonuclear rates have presented unsuspected intellectual rewards in nuclear physics itself. Let us briefly recount some aspects of the general problem.

The adjective *thermonuclear* is chosen to reflect the fact that the countless scatterings per reaction inside a star maintain a thermal distribution of particle states. For a Maxwellian two-particle distribution, the probability that the relative velocity of a pair has magnitude v in the interval dv is

$$\phi(v, T)\, dv = \left(\frac{M}{2\pi kT}\right)^{3/2} \exp\left(-\frac{Mv^2}{2kT}\right) 4\pi v^2\, dv,$$

* Invited talk: International Conference on Nuclear Physics, Munich, August, 1973. [Published in *Proceedings of the International Conference on Nuclear Physics in Munich, August, 1973* (North Holland, Publ. Co., Amsterdam, 1974)].

† Present Address: Kellogg Radiation Laboratory, California Institute of Technology, Pasadena, California.

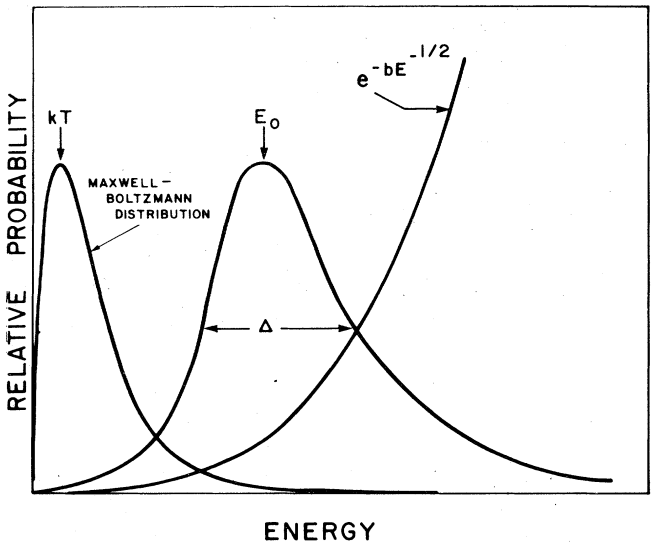

FIG. 1. The most effective energy range $E_0 \pm \Delta E_0/2$ in a charged-particle channel relying on thermal energy (whether incident channel or endoergic exit channel) is a compromise between the Maxwellian tail and the Gamow–Gurney–Condon penetration factor. The most effective energy E_0 increases with charge and temperature (Clayton, 1968).

where M is the reduced mass of the pair (Clayton, 1968). The reaction rate at temperature T is then

$$r(T) = N_1 N_2 \int_0^\infty \sigma(v) v \phi(v,T)\, dv = N_1 N_2 \langle \sigma v \rangle ,$$

where N_1 and N_2 are the densities of interacting particles, and $\sigma(v)$ is the cross section for the reaction as a function of the relative velocity. The traditional problem occurs because the density of interacting pairs drops exponentially in the interaction energy. The Gamow factor in the barrier penetration is proportional to

$$P(v) \propto \exp(-2\pi Z_1 Z_2 e^2/\hbar v) = \exp(-b/E^{1/2})$$

which is virtually zero at thermal energies except for neutrons. Figure 1 shows the traditional compromise, wherein the product of these two factors results in a "most effective energy" E_0:

$$E_0 = 0.122(Z_1^2 Z_2^2 A)^{1/3} T_9^{2/3}\ \text{MeV},$$

where A is the reduced atomic weight, and $T_9 = 10^{-9}T$ is the temperature in billions of degrees. There is a range of effective energies ΔE_0 centered on E_0 with width

$$\Delta E_0 = 0.237(Z_1^2 Z_2^2 A)^{1/6} T_9^{5/6}\ \text{MeV}.$$

Outside this range of energies the cross section is of comparatively little interest. These simple considerations apply if the Q of the reaction allows it to proceed at these energies and if there does not exist a more severely energy-dependent Coulomb barrier in the exit channel. Consider some examples of the types of studies that one is up against.

A. $^{12}C(p, \gamma)^{13}N$. A classic case

This reaction is a part of the CN cycle, and at those temperatures occurs primarily at energies between 15 keV and 50 keV, which is too low to measure. This is the classic Coulomb-inhibited problem. Figure 2 shows the measurements (Fowler, Caughlan, and Zimmerman, 1967) of the cross section factor $S(E)$ obtained after factoring the $\pi\lambda^2$ and the proton penetration factor from the cross section:

$$\sigma(E) = \frac{S(E)}{E} \exp(-2\pi Z_1 Z_2 e^2/\hbar v).$$

Exptrapolation of the smooth behavior of $S(E)$, aided if possible by a model of the reaction (which in this case is just the low-energy tail of a broad resonance), is the best one can do. One can see in Fig. 2 that the extrapolation of the curve to the range of effective stellar energies looks secure, provided only that one obtain auxiliary assurance that no additional low-energy resonances will be encountered. This type of problem is common below atomic weight 20, where the separation of compound-nuclear resonances is generally much greater than E_0.

B. $^{16}O(p, \alpha)^{13}N$. A low-A example from explosive oxygen and silicon burning.

The importance of this reaction was shown by Woosley' Arnett, and Clayton (1972b) to be great in explosive oxygen burning. By influencing the various modes of destruction of ^{16}O, it determines to a great extent the amount of nucleosynthesis in the mass range $A > 28$ relative to that of $A = 28$. It is also of importance in silicon burning. Because the reaction is endoergic by 5.22 MeV, the Coulomb barrier does not affect the protons; instead, their energy must be 5.22 MeV plus the effective energy E_0 for $^{13}N + {}^4He$, which faces Coulomb inhibition in the exit channel. For termperatures in the range $3.0 < T_9 < 5.5$, the most effective $\alpha - {}^{13}N$ energies (including $\Delta E/2$) range from 1.3 MeV to 4.7 MeV, so that incident channel energies of 6.5 to 9.9 MeV contribute significantly to the thermonuclear rate. These are quite measureable, showing one of the pleasant properties of nuclear data needs at high temperatures. Fig (3) shows measurements of this cross section down to 6.31 MeV, obtained by activation techniques of the ^{13}N. This cross section can be numerically integrated for the temperatures of interest. The behavior of the cross section below 6.3 MeV can be approximated by the alpha-particle penetration factor, which is shown as a dashed line on the low energy edge of the measured cross section. Once the integrals have been done for many temperatures, the effective thermonuclear cross section can be adequately approximated by a simple function of temperature, as Woosley (1973) has done in this case.

C. Reverse reactions

If it were not for the fact that ^{13}N is unstable, the thermonuclear rate for $^{16}O(p, a)^{13}N$ could have been measured in the opposite direction. In thermonuclear rates, the relevant energy range in the compound nucleus is the same regardless of the direction of the reaction; i.e., the $^{13}N(\alpha, p)^{16}O$ reaction would be of interest between 1.3 and 4.7 MeV. Many reaction rates to be listed later will be more easily

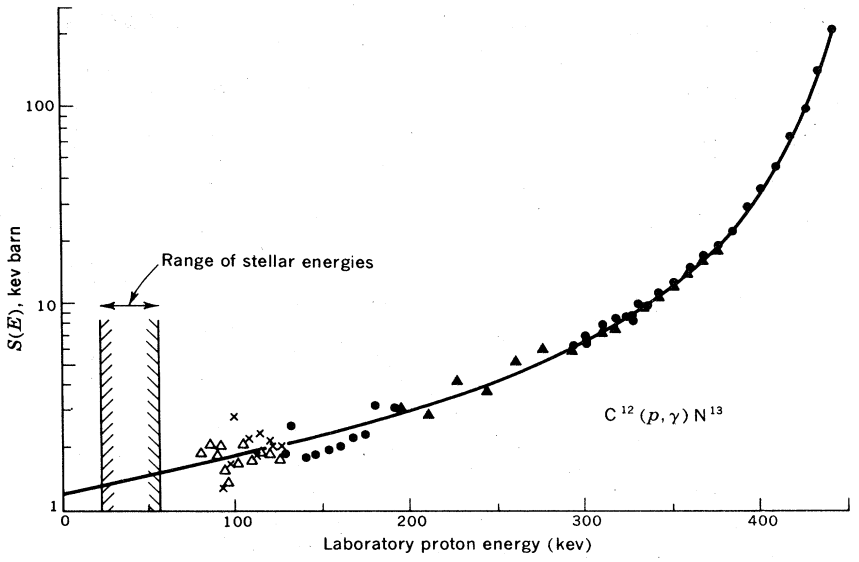

FIG. 2. Cross-section factor $S(E)$ for the radiative capture of protons by ^{12}C. The different types of data points represent five different experiments. Since the curve is a semitheoretic fit to a broad resonance, the continued extrapolation to stellar energies looks secure.

measured in the opposite direction to that of their occurrence in stars, so it is essential to appreciate this reciprocity. Indeed, many reactions occur in *both* directions in stellar explosions.

The quantum principles of reciprocity relate the cross section for $1 + 2 \rightarrow 3 + 4 + Q_{12,34}$ to the cross section $3 + 4 \rightarrow 1 + 2 - Q_{12,34}$:

$$(2J_1 + 1)(2J_2 + 1)\frac{\sigma(12,34)}{\lambda\!\!\!^{-}_{12}{}^2} = (2J_3 + 1)(2J_4 + 1)\frac{\sigma(34,12)}{\lambda\!\!\!^{-}_{34}{}^2}.$$

If only ground states of the reactants enter, one easily shows that the thermal average $\langle\sigma v\rangle_{12,34}$ for a reaction is proportional to the thermal $\langle\sigma v\rangle_{34,12}$ for the inverse reaction:

$$\langle\sigma v\rangle_{34,12} = \langle\sigma v\rangle_{12,34}\left(\frac{M_{12}}{M_{34}}\right)^{3/2}\frac{(2J_1 + 1)(2J_2 + 1)}{(2J_3 + 1)(2J_4 + 1)} \cdot \exp\left(-\frac{Q_{12,34}}{kT}\right),$$

where M is the reduced mass of the channel.

For nuclei having a high density of states, the situation is considerably more complicated. There are two reasons for this: (1) in laboratory measurements, the reacting particles in the entrance channel are in their ground states, whereas in the star they are thermally distributed among all states according to the Boltzmann principle; (2) even if reactants are in their ground states, the stellar problem requires the *total* reaction cross section, which includes excited states in the exit channel. Nonetheless, it is easily shown that if *all* excited states are taken into account in both channels, the above equation remains correct provided the statistical factor $(2J + 1)$ for each nucleus is replaced by the nuclear partition function

$$G = \sum_i (2J_i + 1)\exp(-E_i/kT)$$

for each nucleus, where the sum is over the states (J_i, E_i) of the nucleus. A very relevant example is the reaction $^{24}Mg(\alpha, p)^{27}Al$, which occurs both ways during explosive oxygen burning and explosive silicon burning, and is measurable in either direction.

D. $^{27}Al(p, \gamma)^{28}Si$. Many narrow resonances and photodisintegration

During explosive oxygen and silicon burning, this reaction occurs at proton energies between 0.5 and 3.2 MeV. It also is of importance in both directions. In this range of energies there are many narrow proton resonances. If the partial widths are roughly constant over a narrow resonance, its cross section

$$\sigma = \frac{2J + 1}{(2J_1 + 1)(2J_2 + 1)}\pi\lambda\!\!\!^{-}_{12}{}^2\frac{\Gamma_{12}\Gamma_{34}}{(E - E_r)^2 + (\Gamma/2)^2}$$

can be integrated with the thermal distribution:

$$\langle\sigma v\rangle_r \approx [v\phi(v,T)]_{E=E_r}\int_0^\infty \sigma(v)\,dv = \hbar^2\left(\frac{2\pi}{MkT}\right)^{3/2}\frac{2J + 1}{(2J_1 + 1)(2J_2 + 1)}\frac{\Gamma_{12}\Gamma_{34}}{\Gamma} \cdot \exp-\left(\frac{E_r}{kT}\right).$$

The contribution of each resonance to $\langle\sigma v\rangle$ can either be measured in the laboratory directly, or calculated if the relevant parameters describing the resonance are known. Often only a single width need be known, because the total width Γ will in some cases be dominated by the larger of the two channel widths, in which case it cancels.

The solid curves in Fig. 4 show the measured yield (Lyons, Toevs, and Sargood, 1969) of this reaction as a function of laboratory proton energy. The many narrow (compared with ΔE_0) resonances are evident. The reaction area under each must be measured or calculated. These

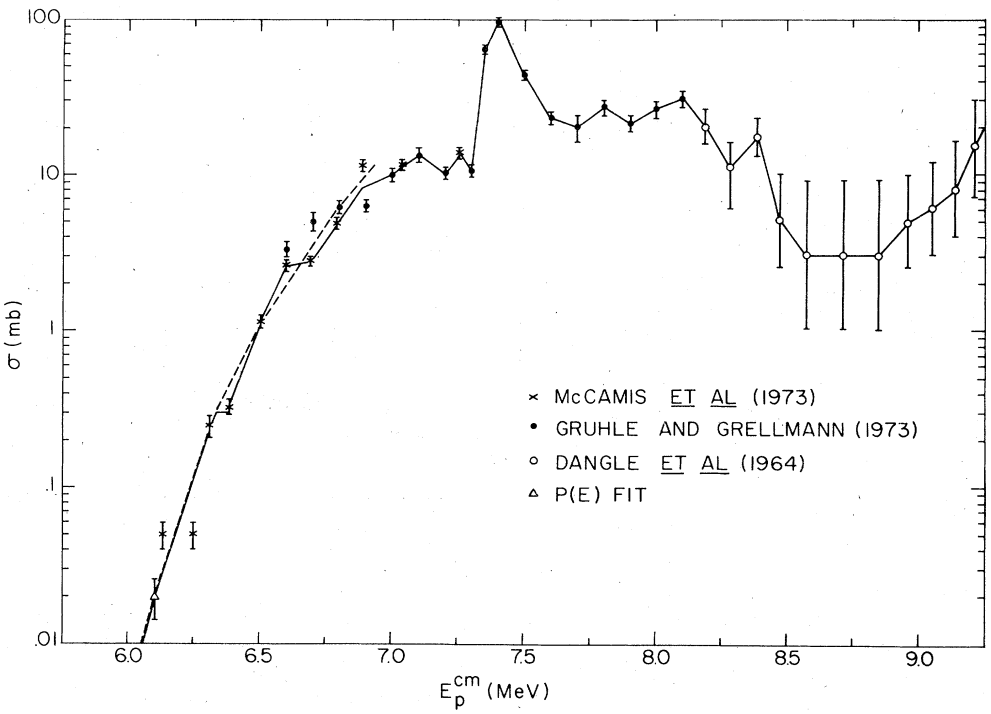

FIG. 3. Cross-section for $^{16}O(p,\alpha)^{13}N$ as a function of energy. The sources of data are given by Woosley (1973), whose dashed line at lowest energies reflects the shape of the alpha-particle penetration factor. Most of the thermonuclear reaction rate, however, comes from numerical integration of the measured cross section.

spectra were taken with a Moxon-Rae-type gamma detector which sums the gamma cascade, thereby automatically summing the gamma widths to all excited states, as needed for the total radiative cross section. Also shown as a dashed curve is the continuum cross section (measured in μbarns on the right hand ordinate). The contribution of the continuum to $\langle\sigma v\rangle$ can be obtained by simple numerical integration. This type of study is typical of what is needed in the intermediate mass region. In addition to solving this specific problem, it provides valuable guidance to nuclear systematics in this mass range.

What is needed in silicon burning is the inverse $^{28}Si(\gamma, p)^{27}Al$ reaction. When averaging over the Planck spectrum and the excited states of target ^{28}Si, the thermonuclear photodisintegration rate is (for the general reaction $\gamma + 3 \rightarrow 1 + 2$)

$$\lambda_\gamma(3) = \left(\frac{M_{12}kT}{2\pi\hbar^2}\right)^{3/2} \frac{G_1G_2}{G_3} \exp\left(-\frac{Q_{12,3\gamma}}{kT}\right) \langle\sigma v\rangle_{12,3\gamma}.$$

The measurements in Fig. 4 included the gamma cascades to all excited states, so it can be inverted directly provided that excited states of ^{27}Al do not participate in the reactions. That assumption is not correct. Those states are suppressed in importance, however, by the steep exponential of the Boltzmann distribution, unlike the excited states of ^{28}Si, which, though greater in excitation energy, do not increase the energy that must be borrowed from the thermal distribution to drive the $^{28}Si(\gamma, p)^{27}Al$ reaction. This makes the excited states of ^{28}Si instrinsically more important that those of ^{27}Al. Nuclear factors also enter, however, and one notes, for instance, that s-wave protons can form 0^+ states with the $1/2^+$ first excited state of ^{27}Al at 0.84 MeV, whereas they cannot with the $5^+/2$ ground state. Although this is not so important for the radiative channel, it may be important for the $^{24}Mg + {}^4He$ channel.

E. $^{51}V(n, \gamma)^{52}V$. A neutron reaction

The distinguishing feature of neutron-induced thermonuclear reactions is the absence of the Coulomb barrier in that channel: and in this particular example there is no Coulomb barrier in either channel. In such a case the neutron cross section is most important near the peak of the thermal distribution $[kT = 86T_9keV]$. The most extensive application of (n, γ) reactions has been in the s-process (Clayton *et al.*, 1961) capture chains in the heavy elements. Allen, Gibbons and Macklin (1971) and Macklin and Gibbons (1965) have given a recent reappraisal of the cross section information there. In these cases it is useful to define an average thermal cross section $\langle\sigma(kT)\rangle$ having the property that its product with the most probable thermal velocity $v_T = (2kT/M)^{1/2}$ equals $\langle\sigma v\rangle$:

$$\langle\sigma(kT)\rangle = \frac{1}{v_T}\int_0^\infty \sigma(v)v\phi(v,T)\,dv\,.$$

It is not necessary to have high-energy resolution in these experiments because of the required average over thermal energies to be made in any case.

Figure 5 shows the data for the neutron magic nucleus ^{51}V. The cross section shows a lot of structure. The solid curve, by contrast, shows the thermally averaged cross section $\langle\sigma(kT)\rangle$ on the same energy scale. One sees that

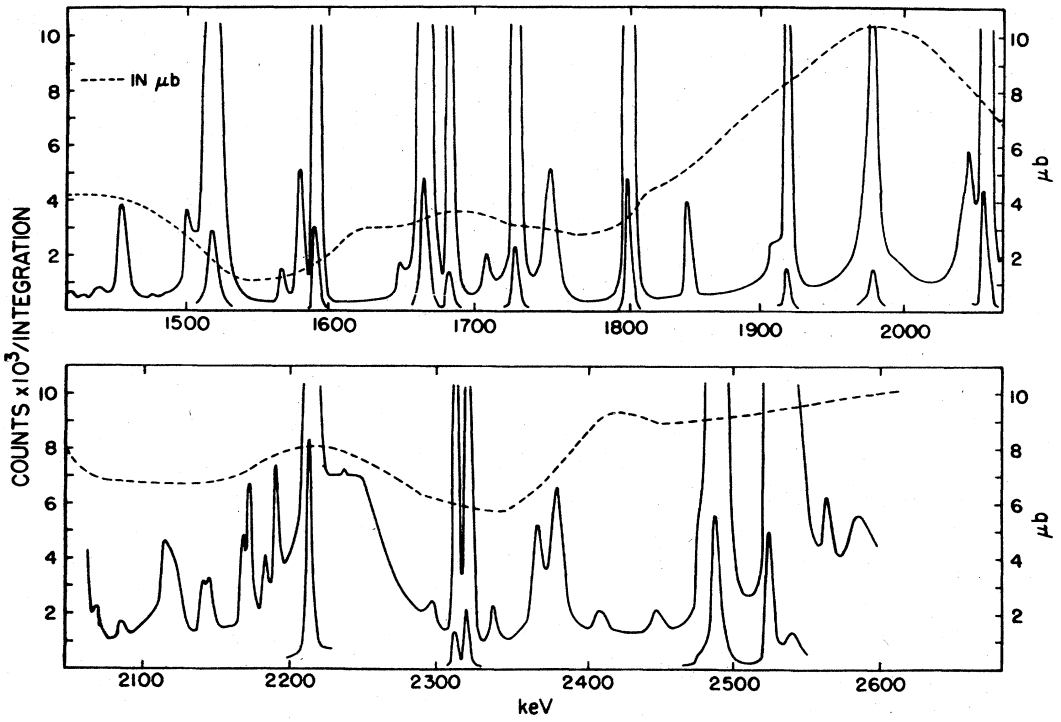

FIG. 4. Relative yield of resonances observed (Lyons, Toevs, and Sargood, 1969) in the $^{27}Al(p,\gamma)^{28}Si$ reaction. Each resonance provides a "capture area" for the thermonuclear average. The nonresonant cross section is shown as a dashed curve whose values in μbarns is on the right-hand ordinate.

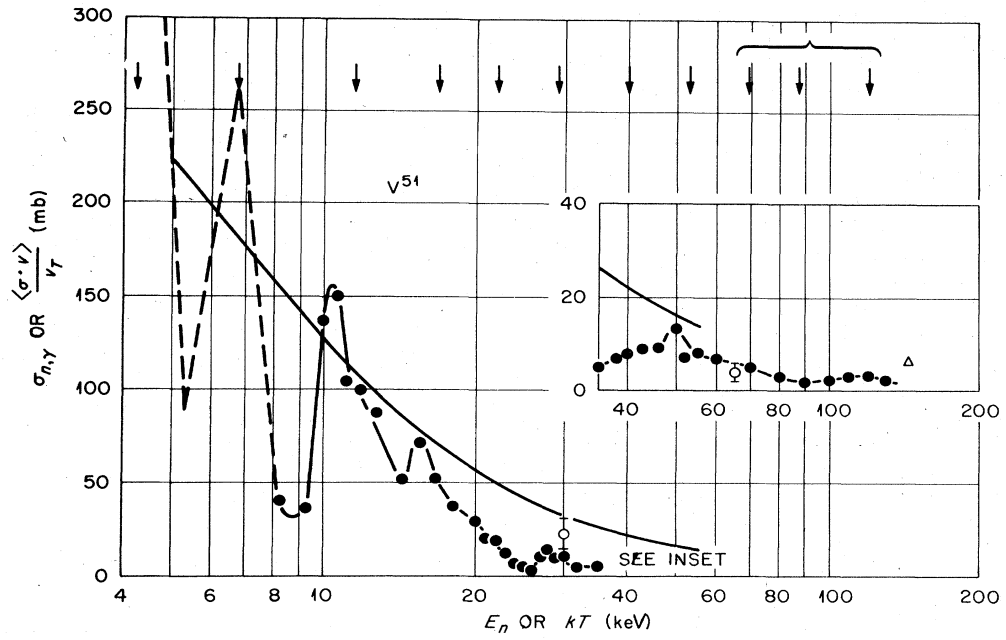

FIG. 5. Neutron-capture cross section of the neutron magic nucleus ^{51}V. The connected points represent measured values $\sigma(E_n)$, and the arrow across the top show the position of neutron resonances known (Macklin and Gibbons, 1965) from the total cross section. The smoothly falling solid curve shows $[\sigma(kT)]$.

a measurement of the cross section at E_n does not give a good measure of the thermal cross section at $kT = E_n$. In heavier nuclei, on the other hand, there is not so much structure in the tens-of-kilovolts region, so that measurement at E_n can provide a good measure of $\langle\sigma\rangle$ at $kT = E_n$. An analysis can then be made in terms of s-and-p-wave strength functions and the ratio of radiative width to level spacing (Macklin and Gibbons, 1965; Michaud and Fowler, 1970).

A different problem occurs in the $^{24}Mg(n,\alpha)^{21}Ne$ reaction in explosive silicon burning. It is endoergic by 2.65 MeV,

and the outgoing alpha must lie in the effective range $E_0 \pm \Delta E_0/2$. Thus it works out that neutron energies in the range 4.5–8.4 MeV are relevant. In this case, moreover, one might prefer to measure the inverse $^{21}Ne(\alpha, n)^{24}Mg$ reaction for alpha energies between 1.9 MeV and 5.8 MeV.

These examples only scratch the surface. Each reaction is a special problem unto itself, and can be a delight to the man who cares about the answer. An especially good technical discussion of thermonuclear reaction rates has been presented by Michaud and Fowler (1970). A good survey of the special experimental problems can be found in the report *New Uses for Low-Energy Accelerators* (National Accademy of Sciences, 1968). Se let us turn to some of the modern applications to astronomical problems, after which we will tabulate the needed cross sections, which, hopefully, will have been illuminated by these examples.

III. THERMONUCLEAR REACTIONS: STELLAR EVOLUTION AND NUCLEOSYNTHESIS

Throughout the 1950's and 1960's emphasis in nuclear astrophysics lay on static stars. Astronomers and astrophysicists discovered that the assumption that stars change very slowly allowed the equations governing stellar structure to be easily solved on a computer. This assumption was consistent with the nonchanging appearance of the majority of the stars. Nuclear physicists, led by those at the California Institute of Technology, made laborious and careful measurements of the cross sections for the nuclear reactions that provide the thermonuclear power for static stars. It was found that models of stars build up spherical shells of differing composition as the interiors burn successively through the stages of available nuclear fuel–hydrogen burning, helium burning, carbon burning, oxygen burning, and silicon burning. These calculations illuminated the details of the slow evolution of the star, and it was often tacitly assumed that the nuclear ashes of these epochs would provide an understanding of the observed abundances of the elements. It is now believed that the last assumption is oversimplified. The natural abundances of most of the nuclei may have been established in a few final seconds of the star's lifetime as it explosively disrupts. The nuclear reactions burn so furiously at the high temperature of the explosion that the composition of the entire star is altered. There are, however, several important nuclei that *are* produced by the static evolution of the star and that either simply *survive* the final explosion or are returned to the interstellar medium when the star quietly loses a significant fraction of its mass. These nuclei are probably only H, He, ^{12}C, ^{14}N, ^{16}O, ^{22}Ne and the *s*-process nuclei.

The hydrogen itself is regarded as primeval, in the sense that it existed as the dominant species before stars and galaxies were born. Static hydrogen burning rather than a big bang may be the source of ^4He in nature, although most evidence suggests the helium already existed when galaxies formed. Certainly the overwhelmingly dominant source of stellar thermonuclear power is the fusion of hydrogen into helium, either by the proton–proton chains or by the carbon–nitrogen cycle. Perhaps the high rates of this conversion in massive stars early in the lifetime of the Galaxy produced most of the galactic ^4He. The burning via proton–proton chains in the outer layers of stars may be the natural source of ^3He as well. Because the CN cycle converts initial amounts of carbon and oxygen into ^{14}N, which is difficult to make by other means, it seems certain that ^{14}N is somehow ejected from stars without being completely destroyed. Some ^{13}C may also result from these reactions. This CNO conversion can work effectively as soon as the very first stars have synthesized ^{12}C and ^{16}O from ^4He, because that ^{12}C and ^{16}O will be mixed into later forming stars. The large N/C ratios in some evolved stellar surfaces show the results of $^{12}C \rightarrow {}^{14}N$ conversion in their interiors.

When the hydrogen is exhausted by static burning, the subsequent contraction ignites ^4He fusion into ^{12}C and ^{16}O. The great abundance of these two nuclei is due to the fact that they are not largely destroyed in the final explosions. The ^{14}N left from the CN cycle is converted largely to ^{22}Ne during the helium burning epoch, and its survival of the explosion is believed to be the origin of ^{22}Ne.

The other important class of surviving nuclei are those produced by the slow capture of free neutrons liberated during the evolution of the static star. The process is commonly called the *s*-process (Clayton *et al.*, 1961), and the nuclei believed to be produced in this way are of relatively low abundance–most having atomic weight considerably greater than iron (Peters, Fowler, and Clayton, 1972). It was the great overabundances of these *s*-process nuclei, particularly Sr, Zr, and Ba observed in certain classes of evolved stars that provided one of the strongest historical motivations for nucleosynthesis in stars. It observationally proved stellar interiors to be thermonuclear reactors. Somehow, these evolved stars lose their enriched envelopes and with them numerous *s*-process nuclei. This mode of nucleosynthesis must happen in static rather than exploding stars, moreover, because it must happen slowly enough to allow beta decays to occur following the neutron captures. The correctness of this theory has been demonstrated by careful measurements of neutron-capture cross sections at the Oak Ridge National Laboratory (Allen, Gibbons, and Macklin, 1971). Because the rate of destruction of each successive nucleus A in the chain of neutron captures is proportional to $\sigma_A(n,\gamma)$, the abundance produced is inversely proportional to $\sigma_A(n,\gamma)$. The degree of success is best illustrated by two isotopes of samarium, ^{148}Sm and ^{150}Sm, whose abundances are believed for other reasons to be overwhelmingly due to the *s* process. The measured values for the products of the abundance and neutron-capture cross section stand in the ratio (Allen, Gibbons, and Macklin, 1971)

$$\frac{N(^{148}Sm)}{N(^{150}Sm)}\frac{\sigma(^{148}Sm)}{\sigma(^{150}Sm)} = 0.98 \pm 0.06$$

which is convincingly near the expected value of unity. The theory has many successes of this type and, to date, no failures, so it must be regarded as confirmed beyond reasonable doubt. Many (n, γ) cross sections in the chain need measuring, and the reader is referred to Allen, Gibbons, and Macklin (1971) for the current status of the problem. We will not consider it further here, because we wish to turn to the main burden of this review.

By the mid 1960's it was becoming clear that highly evolved massive stars were potentially quite explosive—that if the temperature of zones of carbon and oxygen were

suddenly increased by 50% a thermonuclear explosion would disrupt the entire star. Largely due to the intense neutrino losses that cause evolved stars to be more centrally condensed than had previously been supposed, the stellar models seem to approach an explosive instability. Hydrodynamic computations of the explosive event have only recently begun, but it now seems that the several spherical shells of evolved stars will be dramatically compressed and heated during the explosive event. The high temperature of the nuclear explosion, which lasts only a fraction of a second, produces such a high degree of nuclear processing that the expelled thermonuclear products are vastly different than the composition of the mass zones before the explosion. The natural abundances of the elements provide convincing testimony to the fact that many of them were synthesized in just such events. The recent dramatic progress in this aspect of the science stems from the realization that the composition of the entire star probably changes in a few explosive terminal seconds and from the development of accurate numerical computation programs for the networks of nuclear reactions that proceed during the explosion. The results of these explosive chains of nuclear reactions can now be seen to be virtually identical to the observed abundance of a subset of the elements and their several isotopes.

The left hand side of Fig. 6 shows schematically the spherical shell structure of the composition of a typical evolved star having a mass 10 to 60 times the mass of the sun. Proceeding inward from the surface we reach a sufficiently high temperature at the base of zone I that the hydrogen is fusing into helium. Within that point (zone II) the hydrogen is already exhausted and helium is the dominant species. The only other major nucleus in zone II is ^{14}N, which was produced by the CN cycle from the small concentration (about 2% by mass) of ^{12}C and ^{16}O that was initially present in the star. At the base of zone II the temperature is sufficiently high that helium is fusing into ^{12}C and ^{16}O, which are the main constituents of zone III in which the helium is already exhausted. The 2% of ^{14}N has been simultaneously converted to ^{22}Ne by two successive (α, γ) reactions, and both the ^{14}N and ^{22}Ne owe their existence to partial survival within these zones when they are ejected. At the base of zone III the carbon fuses into ^{20}Ne, ^{24}Mg, and ^{23}Na (in order of abundance), and the ^{22}Ne has been converted to heavy isotopes of magnesium. In zone IV the weakly bound ^{20}Ne is converted to ^{16}O and ^{24}Mg, which are the two dominant species of that zone. The ^{16}O is fusing at the base of zone IV. In zone V the oxygen has already burned in the previous static evolution and ^{28}Si and ^{32}S are major nuclear species. In the central zone the silicon is being converted into nickel and iron. In each of these zones remains the very small concentrations (about 10^{-3} by mass) of heavy elements that were initially present in this star. This may provide important seed nuclei at the time of the explosion of the main fuels.

This then may be the situation just before the rapid contraction of the central zone causes the overlying layers to be compressionally heated to such a point that they explode. It is the *presupernova structure* for one class of models for such events—namely the class of massive star models responsible for the nucleosynthesis of most nuclei. The right hand half of Fig. 6 indicates as "explosive products" the major nuclei synthesized during the explosion, and it also indicates the major "survivors" discussed previously. It is not yet known with certainty what fraction of survivor class nuclei actually survive *the explosion* as opposed to their survival from outer zones of stars that *lose mass more gently.*

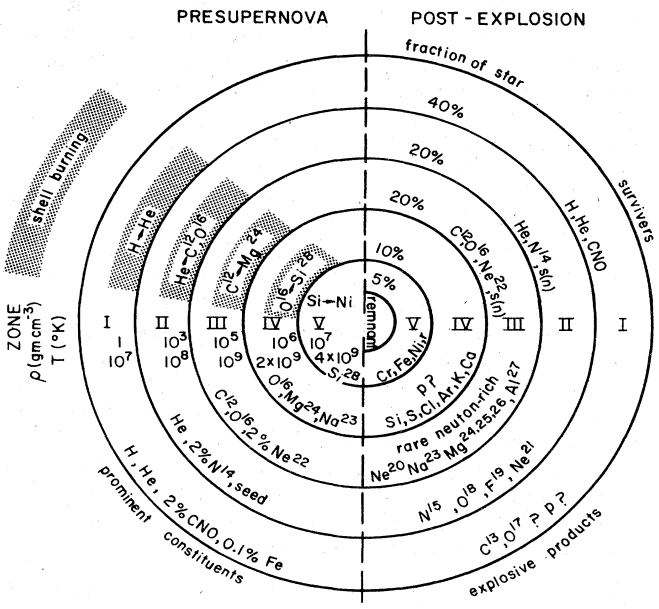

FIG. 6. A schematic diagram of the structure and composition of a massive star prior to its explosive disruption is shown to the left of the central dashed line, and the postexplosion composition is shown to the right. The zones are identified by roman numerals, and the pre-explosion temperature and density are also suggested. Both the nuclei surviving the explosion after earlier synthesis and the nuclei synthesized during the explosion are shown in the right half.

No one has yet actually calculated the (numerical) hydrodynamics of an exploding object similar to Fig. 6, although Arnett is in hot pursuit of this goal. General physical principles suggest that the combination of compression plus explosive burning will quickly produce a peak energy density whose expansion and cooling will be almost adiabatic. The time scale for the expansion will likely be within an order of magnitude of the free fall time scale for a spherical object of the same density: $\tau_{\rm fall} \approx 446 \text{ sec } [\rho_0(\text{gcm}^{-3})]^{-1/2}$. In studying the nuclear properties, therefore, we have taken the convenient approach that the thermodynamic history of each zone may be specified by characterizing the explosion in terms of an e-fold time for the density

$$\rho(t) = \rho_0 \exp(-t/\tau_{\rm hd}) \text{ gcm}^{-3}$$

with

$$\tau_{\rm hd} = 446 \chi \rho_0^{-1/2} \text{ sec}$$

and χ is an arbitrary scaling parameter (expected to be of order unity) for testing the dependence of the results upon the hydrodynamic time scale $\tau_{\rm hd}$. If the expansion is adiabatic, ρ is approximately proportional to T^3; we have taken that to be exact. Given those symplifying assumptions, the thermonuclear evolution of each zone depends upon the initial (peak) values of temperature and density

and upon the expansion time scale parameter χ. The evolution of the nuclear abundances during the expansion is obtained by integrating numerically the set of coupled nonlinear differential equations. The numeric techniques were set forth by Arnett and Truran (1969). A happy result of this procedure is that the nuclear results can often be understood in simpler and more general terms than simply the result of a numerical experiment. *We have always attempted to identify the effect of the values of nuclear cross sections on the physically significant results, and the main point of this entire paper is to pass on that information.* In many cases the importance of a cross section was determined by simply repeating an integration with a new value for the cross section, but more often than not, its importance could be deduced from intelligent study of the nuclear flows found during an integration. In the Tables to follow, the reason for the importance of each reaction is listed under a column headed "Importance," whereas the value to astrophysics of knowing the exact value of the cross section is listed under a column headed "Value." The meanings of these entries are as follows:

MBR Main burning reaction—affects rate of primary burning or Ptyensi of free particles

$\delta(^{23}\mathrm{Na})$ Cross section affects final abundance of ^{23}Na

$\delta(\eta)$ Cross section affects number of excess neutrons per nucleon of matter

n, *p* Provides free neutrons, protons

qe Reactions established quasiequilibrium

1 Top value—cross section controls a major result

2 Cross section value has direct influence on observable result—measurements important

3 Cross section measurements desirable because value has measurable affect on observable result

4 Cross section measurement useful because it has mild influence on observable result

Cross section importance is entered only for those burning phases where its value is deemed of importance. A given reaction may also occur in a burning phase for which it is not entered, but in that case the omission is because we believe its value to be unimportant there. For example, $^{36}\mathrm{Ar}(p,\gamma)^{37}\mathrm{Cl}$ occurs rapidly during explosive silicon burning, but the value of its cross section is probably not of measurable importance there, so it is not listed.

One additional point should be made again at this time. *All evaluations of thermonuclear reaction rates are important*, even if the reaction is of negligible importance to astrophysics, because every reduction of raw nuclear data to a thermonuclear rate provides added guidelines to the general problem of thermally averaged cross sections. This is especially true in the range of intermediate masses, where both continuum strength and many resonances contribute to the problem. Many thermonuclear rates must be calculated from nuclear systematics in any case, and all careful measurements add to that body of systematics. The approximate energy range of interest for the charged particle reactions listed in these tables is taken as $E_0 \pm \Delta E_0/2$ over the relevant range of temperatures, although that prescription somewhat overestimates the energies at the highest temperatures where the dominant penetration factor is no longer of the Ganow form.

We have left all weak decays out of the table of important reactions. This is not because weak decays are not important. On the contrary, they are quite important, but in the problems we are considering, they are often reasonably well known or calculable. We have simply chosen to concentrate on the strong reactions. Before using the tables, one may consider the following general comments on the burning phases considered in the tables.

A. Hydrogen burning

The reactions of hydrogen burning, the proton–proton chains and CNO cycles, are the oldest and best studied of all the systems of nuclear astrophysics, including their important role in stellar evolution and in the solar neutrino experiment. For that reason we will not discuss them here, referring instead to existing reviews (Clayton, 1968; Fowler, Caughlan, and Zimmerman, 1967; Barnes, 1971). We remark only that these burning phases occur at such low temperatures that the reactions cannot be measured in the energy regson of applicability, so that standard extrapolations like that discussed earlier for $^{12}\mathrm{C}(p,\gamma)^{13}\mathrm{N}$ must be used. As far as nucleosynthesis is concerned, hydrostatic burning is the main natural source of ^{14}N and a heavy producer of ^{4}He; moreover, it is a possible source of ^{3}He and ^{7}Li in the outer layer of evolved stars (Cameron and Fowler, 1971). Howard, Arnett, and Clayton (1971) calculated that explosive ejection of hydrogen could make a natural source of ^{13}C, ^{17}O, and perhaps ^{15}N if the proton density is high enough to allow a substantial fraction of ^{12}C nuclei to capture a proton. The common nova outburst may provide the explosive hydrogen setting for the synthesis of some of these nuclei (Starrfield *et al.*, 1972) any may even provide nuclear gamma rays to prove it (Clayton and Hoyle, 1974).

B. Helium burning and the explosive ejection of helium

Hydrostatic helium burning is extremely important in stars. It is a source of power in stellar evolution, the probable site of the *s* process, and determines the abundance ratio $^{12}\mathrm{C}$:$^{16}\mathrm{O}$:$^{20}\mathrm{Ne}$ for future burning. The last is crucial, because many conclusions regarding stellar evolution and explosive nucleosynthesis hinge on the final abundance ratios when helium is exhausted. Unfortunately the main burning reactions, 3α and $^{12}\mathrm{C}(\alpha,\gamma)^{16}\mathrm{O}$, are not directly measurable, so their rates have been major objectives for nuclear astrophysics (Fowler, Caughlan, and Zimmerman, 1967; Barnes, 1971). The latter remains the most important uncertain cross section in nuclear astrophysics. The reactions of importance during hydrostatic helium burning are listed in Table I under the column labeled *HyHe*. Other than the direct synthesis of ^{12}C and ^{16}O, these reactions are mainly of interest for neutron liberation for the *s* process, synthesis of ^{21,22}Ne from ^{14}N, and the increase in excess neutrons η by the positron emission of ^{18}F.

A second set of columns designates the important reactions and the value of knowing their rates that occur when helium zones are explosively ejected from a star. Howard, Arnett, and Clayton (1971) have evaluated this problem when the helium is compressed to temperature $4 < T_8 < 10$, which is the range of temperatures they found to give interesting and useful results. Because the expansion time is several seconds, the helium cannot fuse with itself via the slow 3α reaction; however, there is a chain of interesting

TABLE I. Reactions important during hydrostatic helium burning ($1 \leq T_8 \leq 8$) and during explosive ejection of helium ($4 < T_8 < 10$).

Reaction	Q (MeV)	Energy Range (MeV)	Importance		Value	
			HyHe	ExHe	HyHe	ExHe
3α	7.37	0.10–0.82	MBR		1	
$^{12}C(\alpha,\gamma)^{16}O$	7.16	0.15–1.1	$\delta(^{16}O)$		1	
$^{12}C(^{12}C,n)^{23}Mg$	−2.62	threshold	neutrons		4	
$^{13}C(\alpha,n)^{16}O$	2.21	0.15–1.3	neutrons	n,$\delta(^{18}O)$	2	4
$^{14}C(\alpha,\gamma)^{18}O$	6.23	0.35–1.3		$\delta(^{18}O)$		3
$^{14}N(p,\gamma)^{15}O$	7.29	0.13–0.66		$\delta(^{15}N^{18}O)$		2
$^{14}N(\alpha,\gamma)^{18}F$	4.42	0.17–1.4	$\delta(^{22}Ne)$	$\delta(^{18}O)$	2	1
$^{14}N(n,p)^{14}C$	0.63	≥ 0		$\delta(^{18}O)$		3
$^{15}N(p,\alpha)^{12}C$	4.97	0.13–0.66		$\delta(^{15}N)$		4
$^{15}O(n,p)^{15}N$	3.54	≥ 0		$\delta(^{15}N)$		4
$^{15}O(\alpha,\gamma)^{19}Ne$	3.53	0.45–1.5		$\delta(^{19}F)$		2
$^{16}O(\alpha,\gamma)^{20}Ne$	4.73	0.20–1.6	$\delta(^{20}Ne)$	$\delta(^{21}Ne)$	2	3
$^{18}O(p,\alpha)^{15}N$	3.98	0.14–0.71		$\delta(^{18}O^{15}N)$		3
$^{18}O(\alpha,\gamma)^{22}Ne$	9.67	0.19–1.5	$\delta(^{22}Ne)$	$\delta(^{22}Ne)$	2	4
$^{18}O(\alpha,n)^{21}Ne$	−0.70	0.70–1.5	n	$\delta(^{18}O^{21}Ne)$	3	4
$^{18}F(\alpha,p)^{21}Ne$	1.74	0.50–1.6		$\delta(^{21}Ne)$		1
$^{19}Ne(\alpha,p)^{22}Na$	2.07	0.55–1.7		$\delta(^{19}F^{22}Ne)$		3
$^{20}Ne(\alpha,\gamma)^{24}Mg$	9.32	0.23–1.5	$\delta(^{20}Ne)$		3	
$^{20}Ne(p,\gamma)^{21}Na$	2.43	0.18–0.81		$\delta(^{21}Ne)$		3
$^{21}Ne(\alpha,n)^{24}Mg$	2.56	0.23–1.7	$\delta(^{21}Ne)$,n	$\delta(^{21}Ne)$	2	4
$^{21}Ne(\alpha,\gamma)^{25}Mg$	9.89	0.23–1.7	$\delta(^{21}Ne)$	$\delta(^{21}Ne^{25}Mg)$	3	4
$^{21}Ne(p,\gamma)^{22}Na$	6.74	0.18–0.81		$\delta(^{21,22}Ne)$		3
$^{22}Ne(\alpha,n)^{25}Mg$	−0.48	0.48–1.5	neutrons		2	
$^{22}Ne(\alpha,\gamma)^{26}Mg$	10.61	0.23–1.5	$\delta(^{22}Ne)$		3	
$^{22}Ne(n,\gamma)^{23}Ne$	5.19	0.02–0.04	n		2	
$^{22}Na(\alpha,p)^{25}Mg$	3.14	0.59–1.8		$\delta(^{25}Mg)$		2
$^{25}Mg(n,\gamma)^{26}Mg$	11.10	0.02–0.04	n		2	
$^{26}Mg(n,\gamma)^{27}Mg$	6.44	0.02–0.04	n		2	

reactions initiated by the reaction of the alpha particles with ^{14}N, which is about 2% by mass of the matter in zone II. The ^{14}N nuclei that react are converted into ^{15}O, ^{18}F, ^{19}Ne, and ^{21}Ne in ratios close to the solar abundances of ^{15}N, ^{18}O, ^{19}F and ^{21}Ne. It is very likely that these four nuclei owe their natural origin to such zones. Fig. 7 shows selected key reaction rates in this zone, and one can see that the alpha-induced reaction rates build up subsequent to the initial reactions on the seed ^{14}N and ^{13}C. As Table I reveals, there are many interesting reactions occurring here that are worthy of experimental effort. The energy range of interest is accessible here, too, being between 1 to 2 MeV for the secondary alpha reactions. These reactions can be quite important for astrophysics, because the origin of the nuclei they synthesize were long standing puzzles until the work of Howard, Arnett, and Clayton (1971). In their thesis is correct, good measurements of the cross sections may tell something of the hydrodynamic ejection of the helium shells.

C. Carbon burning

The fusion of carbon, initiated by the reactions

$$^{12}C + {}^{12}C \rightarrow \begin{cases} {}^{23}Na + p + 2.238\ \text{MeV} \\ {}^{23}Mg + n - 2.623\ \text{MeV} \\ {}^{20}Ne + \alpha + 4.616\ \text{MeV} \end{cases}$$

is the third great source of power for stellar evolution. It first begins near $T = 10^9$K in the contracting core of a star that has consumed its helium, and later it may occur near the base of zone III in an evolved star (see Fig. 6). Carbon is also the last fuel that can burn at a sufficiently low temperature that the thermal emission of neutrinos will not immediately squander the energy. The main burning reaction above and its sequels maintain the interior heat against photon diffusion, and a hydrostatic burning phase can occur as it did for hydrogen and helium fuels. These

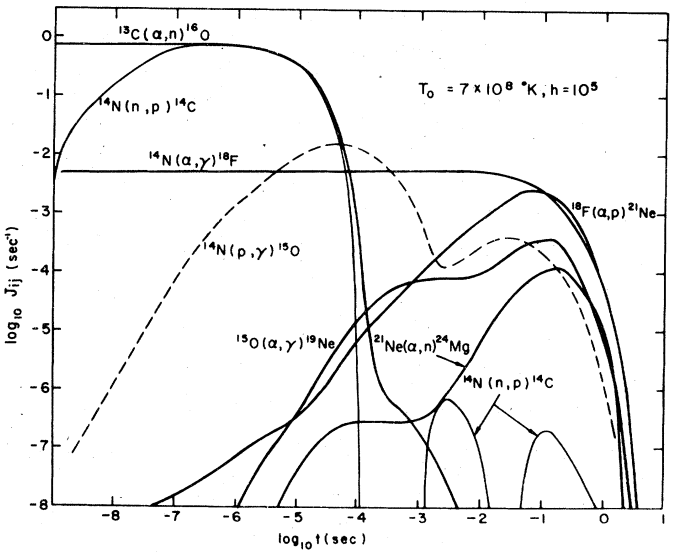

FIG. 7. Selected reaction rates as a function of time during sudden ejection of a helium shell heated initially to 7×10^8°K. Note that the thin solid curve showing the rate of $^{14}N(n,p)^{14}C$ reflects three successive sources of free neutrons: $^{13}C(\alpha,n)^{16}O$, then $^{17}O(\alpha,n)^{20}Ne$, and then $^{22}Ne(\alpha,n)^{25}Mg$. The reaction $^{18}F(\alpha,p)^{21}Ne$ becomes the main source of free protons after the ^{13}C neutron source is exhausted (Howard, Arnett, and Clayton, 1971). Numerical integration of such reaction networks identifies the nuclear reactions of importance to such events

TABLE II. Reactions of importance during hydrostatic carbon burning ($0.6 < T_9 < 1.4$) and explosive carbon burning ($1.8 < T_9 < 2.2$).

Reaction	Q (MeV)	Energy Range (MeV)	Importance		Value	
			HyC	ExC	HyC	ExC
$^{12}C + {}^{12}C$	p,n,α	1.4–5.1	MBR	MBR	1	1
$^{12}C(n,\gamma)^{13}C$	4.95	≥ 0	$\delta(^{16}O)$	$\delta(^{16}O)$	2	2
$^{12}C(p,\gamma)^{13}N$	1.94	0.14–1.1	$\delta(^{16}O,\eta)$,n	$\delta(^{16}O)$	2	3
$^{12}C(\alpha,\gamma)^{16}O$	7.16	0.44–1.6	$\delta(^{16}O)$		4	
$^{13}C(p,\gamma)^{14}N$	7.55	0.14–1.1	$\delta(^{20}Ne)$	$\delta(^{25,26}Mg)$	4	3
$^{13}C(n,\gamma)^{14}C$	8.18	≥ 0	$\delta(^{20}Ne)$	$\delta(^{20}Ne)$	4	3
$^{13}C(\alpha,n)^{16}O$	2.21	0.44–2.2	$\delta(^{16}O)$,n	$\delta(^{16}O)$	2	2
$^{14}C(\alpha,n)^{17}O$	−1.82	1.8–2.2	$\delta(^{20}Ne)$	$\delta(^{20}Ne)$	4	3
$^{14}C(\alpha,\gamma)^{18}O$	6.23	0.44–2.2	$\delta(^{25,26}Mg)$	$\delta(^{25,26}Mg)$	4	4
$^{13}N(n,p)^{13}C$	3.00	≥ 0	$\delta(^{16}O)$	$\delta(^{16}O)$	3	3
$^{13}N(\alpha,p)^{16}O$	5.22	0.51–2.4	$\delta(^{16}O)$	$\delta(^{16}O)$	2	4
$^{14}N(n,\gamma)^{15}N$	10.84	≥ 0	$\delta(^{16}O)$		4	
$^{15}N(p,\gamma)^{16}O$	12.13	0.16–0.85	$\delta(^{16}O)$		4	
$^{15}N(p,\alpha)^{12}C$	4.97	0.16–0.85	$\delta(^{16}O)$		4	
$^{16}O(n,\gamma)^{17}O$	4.14	≥ 0	$\delta(^{16}O^{20}Ne)$	$\delta(^{20}Ne)$	2	2
$^{16}O(p,\gamma)^{17}F$	0.60	0.19–1.3	$\delta(^{16}O)$,n	$\delta(^{20}Ne)$	4	4
$^{16}O(\alpha,\gamma)^{20}Ne$	4.73	0.57–2.6	$\delta(^{16}O^{20}Ne)$	$\delta(^{20}Ne)$	1	3
$^{17}O(\alpha,n)^{20}Ne$	0.59	0.57–2.6	$\delta(^{20}Ne)$,n	$\delta(^{20}Ne)$	3	2
$^{17}O(p,\alpha)^{14}N$	1.19	0.19–0.91	$\delta(\eta)$		2	
$^{17}O(p,\gamma)^{18}F$	5.61	0.32–1.3		$\delta(^{20}Ne)$		4
$^{17}O(n,\alpha)^{14}C$	1.82	≥ 0	$\delta(^{20}Ne)$		4	
$^{18}O(n,\gamma)^{19}O$	3.96	≥ 0	$\delta(^{20}Ne)$		4	
$^{18}O(p,\gamma)^{19}F$	7.99	0.19–0.91	$\delta(^{20}Ne)$		4	
$^{18}O(\alpha,n)^{21}Ne$	−0.70	0.70–2.6	$\delta(^{25,26}Mg)$,n	$\delta(^{25,26}Mg)$,n	4	2
$^{18}O(\alpha,\gamma)^{22}Ne$	9.67	0.58–2.6	$\delta(^{25,26}Mg)$	$\delta(^{25,26}Mg)$,n	3	3
$^{18}O(p,\alpha)^{15}N$	3.98	0.19–0.91	$\delta(^{25,26}Mg)$		3	
$^{18}F(n,p)^{18}O$	2.44	≥ 0	$\delta(\eta)$		2	
$^{18}F(n,\alpha)^{15}N$	6.42	≥ 0	$\delta(\eta)$		2	
$^{18}F(\alpha,p)^{21}Ne$	1.74	0.64–2.1	$\delta(\eta)$		2	
$^{20}Ne(n,\gamma)^{21}Ne$	6.76	≥ 0	$\delta(^{23}Na)$	$\delta(^{23}Na)$	4	3
$^{20}Ne(p,\gamma)^{21}Na$	2.43	0.23–1.4	$\delta(\eta)$	$\delta(^{23}Na)$	2	3
$^{20}Ne(\alpha,\gamma)^{24}Mg$	9.32	0.70–3.0	$\delta(^{20}Ne^{24}Mg)$	$\delta(^{24,25,26}Mg)$	1	2
$^{21}Ne(n,\gamma)^{22}Ne$	10.37	≥ 0	$\delta(^{23}Na)$		4	
$^{21}Ne(p,\gamma)^{22}Na$	6.74	0.23–1.0	$\delta(\eta)$		3	
$^{21}Ne(\alpha,n)^{24}Mg$	2.56	0.70–3.0	$\delta(^{24}Mg)$,n	$\delta(^{24}Mg)$	4	4
$^{21}Ne(\alpha,\gamma)^{25}Mg$	9.89	1.3–3.0		$\delta(^{25}Mg)$		4
$^{22}Ne(p,\gamma)^{23}Na$	8.79	0.23–1.0	$\delta(^{23}Na)$		3	
$^{22}Ne(\alpha,n)^{25}Mg$	−0.48	0.70–3.0	$\delta(^{25}Mg)$,n	neutrons	3	2
$^{22}Ne(\alpha,\gamma)^{26}Mg$	10.61	0.70–3.0	$\delta(^{26}Mg)$,n	neutrons	3	3
$^{21}Na(n,p)^{21}Ne$	4.33	≥ 0	$\delta(\eta)$	$\delta(^{23}Na)$	2	4
$^{22}(Na(n,p)^{22}Ne$	3.63	≥ 0	$\delta(\eta)$		3	
$^{23}Na(n,\gamma)^{24}Na$	6.96	≥ 0	$\delta(\eta)$		1	
$^{23}Na(p,\gamma)^{24}Mg$	11.69	0.25–1.5	$\delta(^{23}Na^{24}Mg)$	$\delta(^{23}Na)$,p	1	2
$^{23}Na(p,\alpha)^{20}Ne$	2.38	0.25–1.5	$\delta(^{23}Na^{20}Ne)$	$\delta(^{23}Na)$,p	1	2
$^{23}Na(\alpha,p)^{26}Mg$	1.82	0.76–3.2	$\delta(^{23}Na^{26}Mg)$	$\delta(^{26}Mg)$,p	2	2
$^{23}Na(\alpha,n)^{26}Al$	−2.96	3.0–3.2		$\delta(^{23}Na^{27}Al)$		4
$^{23}Na(\alpha,\gamma)^{27}Al$	10.09	1.5–3.2		$\delta(^{23}Na^{27}Al)$		3
$^{24}Na(p,n)^{24}Mg$	4.73	0.25–1.1	$\delta(\eta)$		2	
$^{24}Na(\alpha,n)^{27}Al$	3.13	0.76–2.3	$\delta(\eta)$		2	
$^{23}Mg(n,\gamma)^{24}Mg$	16.53	≥ 0	$\delta(\eta)$		3	
$^{23}Mg(n,p)^{23}Na$	4.84	≥ 0	$\delta(\eta)$	$\delta(^{23}Ma)$	2	3
$^{23}Mg(n,\alpha)^{20}Ne$	7.22	≥ 0		$\delta(^{20}Ne)$		4
$^{24}Mg(n,\gamma)^{25}Mg$	7.33	≥ 0	$\delta(^{25,26}Mg)$	$\delta(^{24,25}Mg)$	2	2
$^{24}Mg(\alpha,p)^{27}Al$	−1.60	1.9–3.4	$\delta(^{24}Mg^{27}Al)$	$\delta(^{24}Mg^{27}Al)$	4	2
$^{24}Mg(\alpha,\gamma)^{28}Si$	9.98	0.81–2.5	$\delta(^{24}Mg)$		3	
$^{25}Mg(n,\gamma)^{26}Mg$	11.10	≥ 0	$\delta(^{25,26}Mg)$	$\delta(^{25,26}Mg)$	3	2
$^{25}Mg(p,\gamma)^{26}Al$	6.31	0.27–1.1	$\delta(\eta)$		2	
$^{25}Mg(\alpha,n)^{28}Si$	2.65	0.81–3.4	$\delta(^{25}Mg)$	$\delta(^{25}Mg)$	3	3
$^{25}Mg(\alpha,p)^{28}Al$	−1.20	1.7–3.4		$\delta(^{25}Mg)$		3
$^{26}Mg(n,\gamma)^{27}Mg$	6.44	≥ 0	$\delta(^{26}Mg)$	$\delta(^{26}Mg)$	3	3
$^{26}Mg(p,\gamma)^{27}Al$	8.27	0.27–1.6	$\delta(^{26}Mg^{27}Al)$	$\delta(^{26}Mg^{27}Al)$	2	2
$^{26}Mg(\alpha,n)^{29}Si$	0.03	0.81–3.4	$\delta(^{26}Mg)$	$\delta(^{26}Mg^{29}Si)$	3	2
$^{27}Mg(p,\gamma)^{28}Al$	9.56	0.49–1.6		$\delta(^{29}Si)$		3
$^{27}Mg(\alpha,n)^{30}Si$	4.21	1.6–3.4		$\delta(^{30}Si)$		3
$^{26}Al(n,\gamma)^{27}Al$	13.06	≥ 0	$\delta(\eta)$		3	
$^{26}Al(n,p)^{26}Mg$	4.79	≥ 0	$\delta(\eta)$		3	
$^{27}Al(p,\gamma)^{28}Si$	11.58	0.29–1.7	$\delta(^{27}Al)$	$\delta(^{27}Al)$	2	2
$^{27}Al(n,\gamma)^{28}Al$	7.73	≥ 0		$\delta(^{27}Al)$		3
$^{27}Al(\alpha,p)^{30}Si$	2.38	1.7–3.6		$\delta(^{27}Al^{30}Si)$		2
$^{27}Al(\alpha,n)^{30}P$	−2.65	2.7–3.6		$\delta(^{27}Al)$		4

TABLE II. (Continued).

Reaction	Q (MeV)	Energy Range (MeV)	Importance HyC	Importance ExC	Value HyC	Value ExC
$^{27}Al(\alpha,\gamma)^{31}P$	9.67	1.7–3.6		$\delta(^{27}Al^{31}P)$		4
$^{28}Al(p,n)^{28}Si$	3.85	0.53–1.7		$\delta(^{29,30}Si)$		3
$^{28}Al(\alpha,n)^{31}P$	1.94	1.7–3.6		$\delta(^{31}P)$		4
$^{28}Si(n,\gamma)^{29}Si$	8.48	≥ 0	$\delta(^{29,30}Si)$	$\delta(^{29}Si)$	3	2
$^{29}Si(\alpha,p)^{31}P$	−1.92	2.5–3.7		$\delta(^{31}P)$		2
$^{28}Si(\alpha,\gamma)^{32}S$	6.95	1.8–3.7		$\delta(^{33,34}S)$		3
$^{29}Si(n,\gamma)^{30}Si$	10.62	≥ 0	$\delta(^{29,30}Si)$	$\delta(^{29,30}Si)$	4	2
$^{29}Si(p,\gamma)^{30}P$	5.59	0.57–1.7		$\delta(^{30}Si)$		3
$^{29}Si(\alpha,n)^{32}S$	−1.53	1.8–3.7		$\delta(^{33,34}S)$		3
$^{30}Si(n,\gamma)^{31}Si$	6.59	≥ 0		$\delta(^{30}Si^{31}P)$		4
$^{30}Si(p,\gamma)^{31}P$	7.29	0.57–1.7		$\delta(^{30}Si^{31}P)$		3
$^{31}Si(p,n)^{31}P$	0.69	0.57–1.7		$\delta(^{31}P)$		4
$^{30}P(n,p)^{30}Si$	5.03	≥ 0		$\delta(^{30}Si)$		3
$^{31}P(n,\gamma)^{32}P$	7.94	≥ 0		$\delta(^{31}P)$		4
$^{31}P(p,\gamma)^{32}S$	8.86	0.61–1.8		$\delta(^{31}P)$		2
$^{32}P(p,n)^{32}S$	0.93	0.61–1.8		$\delta(^{33,34}S)$		4
$^{32}S(n,\gamma)^{33}S$	8.64	≥ 0		$\delta(^{33,34}S)$		2
$^{33}S(n,\gamma)^{34}S$	11.42	≥ 0		$\delta(^{33,34}S)$		3
$^{33}S(n,\alpha)^{30}Si$	3.50	0–0.26		$\delta(^{30}Si)$		3

burning regions probably never reach the surface of a star, however, so the nuclear products are not appropriate for direct comparison with natural abundances. Nonetheless the nucleosynthesis that occurs here is very important for other reasons: (1) the star could explode before carbon burning is completed; (2) the change in the number η of excess neutrons per nucleon will effect the debris of any subsequent explosion; (3) the final abundances provide the initial abundances for oxygen burning; and (4) neutron liberating reactions provide a source for the s process. The nuclear details for burning at constant temperature were last analyzed by Arnett and Truran (1969), whose paper makes an excellent guide to the nuclear events. The nuclear reactions playing a role here are listed in Table II.

D. Explosive carbon burning

In the first decisive calculations of explosive nucleosynethesis, Arnett (1969) supposed that the carbon could be made to ignite explosively at temperatures near $T_9 = 2$, which is far in excess of temperatures at which carbon burns in a static object. The carbon and its secondary network of reactions burn furiously for about one-tenth of a second, at which time the reactions freeze. Most of the carbon and virtually all of the initial oxygen remain unburned, and the ejected ratio of synthesized ^{24}Mg to fuel ^{12}C can equal the solar ratio. At the same time, and more significantly perhaps, the nuclei ^{20}Ne, ^{23}Na, $^{24,25,26}Mg$, ^{27}Al, ^{29}Si, and perhaps ^{30}Si and ^{31}P freeze near their solar ratios. The significance of the neutron excess of the gas first becomes apparent here, because the final abundances of nuclei having more neutrons than protons (^{23}Na, $^{25,26}Mg$, ^{27}Al, ^{29}Si primarily) are constrained by the abundances of nuclei having excess neutrons before the explosion (^{18}O and ^{22}Ne primarily, which were synthesized in hydrogen and helium burning from the initial CNO nuclei in the star). Most of these primary products are indicated in zone III of Fig. 6.

The reactions of importance in explosive carbon burning are indicated in Table II also. A great many reactions on the isotopes of Na, Mg, Al, and Si are of considerable importance in determining the final abundances of those isotopes. They also lie at this temperature in an accessible range for measurements; for example, the reaction $^{26}Mg(p,\gamma)^{27}Al$, which is of value 2 in determining the final abundances of ^{26}Mg and ^{27}Al, is of interest in the energy range 0.49 to 1.6 MeV. Those who struggled with the CNO cycle would regard such "high energies" with enthusiasm, but the earlier discussion of the example $^{27}Al(p,\gamma)^{28}Si$ showed new demands that are almost as tough.

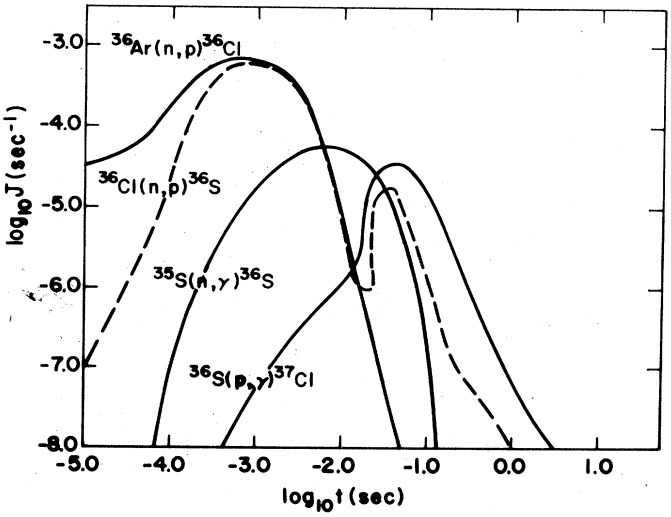

FIG. 8. Some important reaction rates (Howard *et al.*, 1972) involved in the synthesis of ^{36}S from seed nuclei during explosive carbon burning. The early source of ^{36}S is two (n,p) reactions on seed ^{36}Ar nuclei. After ^{36}Ar is exhausted the main source for the $^{36}Cl(n,p)^{36}S$ reaction is the sequence $^{35}S(p,n)^{35}Cl(n,\gamma)^{36}Cl$, where the ^{35}S results primarily from $^{34}S(n,\gamma)^{35}S$. The reaction $^{36}S(p,\gamma)^{37}Ar$ is the main destruction mechanism for ^{36}S, whose natural abundance reveals some details of the explosions of carbon.

TABLE III. Seed reactions of importance during explosive carbon burning ($1.8 < T_9 < 2.2$).

Reaction	Q (MeV)	Energy value (MeV)	Importance	Value
$^{32}S(n,\gamma)^{33}S$	8.64	≥ 0	$\delta(^{36}S)$	2
$^{32}S(n,\alpha)^{29}Si$	1.53	0.4–2.2	$\delta(^{36}S)$	2
$^{33}S(n,\gamma)^{34}S$	11.42	≥ 0	$\delta(^{36}S)$	1
$^{33}S(n,p)^{33}P$	0.53	0.1–1.3	$\delta(^{36}S)$	2
$^{33}S(n,\alpha)^{30}Si$	3.50	0–2.6	$\delta(^{36}S)$	1
$^{34}S(n,\gamma)^{35}S$	6.99	≥ 0	$\delta(^{36}S)$	1
$^{34}S(p,\gamma)^{35}Cl$	6.37	0.6–1.9	$\delta(^{36}S)$	3
$^{35}S(n,\gamma)^{36}S$	9.88	≥ 0	$\delta(^{36}S)$	2
$^{36}S(n,\gamma)^{37}S$	4.42	≥ 0	$\delta(^{36}S)$	4
$^{36}S(p,\gamma)^{37}Cl$	7.96	0.6–1.9	$\delta(A \geq 36)$	1
$^{35}Cl(n,\gamma)^{36}Cl$	8.58	≥ 0	$\delta(^{36}S,^{40}Ar)$	3
$^{35}Cl(n,p)^{35}S$	0.62	0–1.3	$\delta(^{36}S,^{40}Ar)$	3
$^{35}Cl(p,\alpha)^{32}S$	1.86	0.7–2.2	$\delta(^{36}S)$	4
$^{36}Cl(n,\gamma)^{37}Cl$	10.32	≥ 0	$\delta(^{36}S,^{40}Ar)$	2
$^{36}Cl(n,p)^{36}S$	1.92	≥ 0	$\delta(^{36}S,^{40}Ar)$	2
$^{36}Cl(n,\alpha)^{33}P$	2.46	0–1.5	$\delta(^{36}S,^{40}Ar)$	4
$^{37}Cl(n,\gamma)^{38}Cl$	6.11	≥ 0	$\delta(^{36}S,^{40}Ar)$	2
$^{37}Cl(p,\gamma)^{38}Ar$	10.24	0.7–1.9	$\delta(^{36}S,^{40}Ar)$	1
$^{37}Cl(p,\alpha)^{34}S$	3.03	0.7–1.9	$\delta(^{36}S,^{40}Ar)$	1
$^{38-45}Cl(n,\gamma)$	...	≥ 0	$\delta(^{40}Ar,^{40}K)$	3–4
$^{38-45}Cl(p,n)$	...	0.7–1.9	$\delta(A \geq 40)$	3–4
$^{36}Ar(n,\gamma)^{37}Ar$	8.79	≥ 0	$\delta(A \geq 40)$	2
$^{36}Ar(n,p)^{36}Cl$	0.07	0.6–1.9	$\delta(^{36}S)$	1
$^{36}Ar(n,\alpha)^{33}S$	2.00	0–2.1	$\delta(^{36}S)$	3
$^{37}Ar(n,\gamma)^{38}Ar$	11.84	≥ 0	$\delta(A \geq 40)$	4
$^{37}Ar(n,p)^{37}Cl$	1.60	0–3.4	$\delta(A \geq 40)$	1
$^{37}Ar(n,\alpha)^{34}S$	4.63	≥ 0	$\delta(A \geq 40)$	1
$^{38}Ar(n,\gamma)^{39}Ar$	6.59	≥ 0	$\delta(^{40}Ar)$	4
$^{38}Ar(n,p)^{38}Cl$	−4.13	4.8–6.1	$\delta(^{40}Ar)$	4
$^{38}Ar(p,\gamma)^{39}K$	6.37	0.7–2.0	$\delta(^{40}K)$	2
$^{38}Ar(n,\alpha)^{35}S$	−0.22	2.2–4.3	$\delta(^{36}S)$	4
$^{39}Ar(n,\gamma)^{40}Ar$	9.87	≥ 0	$\delta(^{40}Ar,^{40}K)$	3
$^{39}Ar(n,\alpha)^{36}S$	3.06	0–1.0	$\delta(^{36}S)$	3
$^{39}Ar(p,n)^{39}K$	−0.33	0.7–2.0	$\delta(^{40}K)$	3
$^{40}Ar(n,\gamma)^{41}Ar$	6.10	≥ 0	$\delta(^{40}Ar)$	4
$^{40}Ar(p,\gamma)^{41}K$	7.80	0.7–2.0	$\delta(^{40}Ar)$	3
$^{41-44}Ar(n,\gamma)$	...	≥ 0	$\delta(A \geq 43)$	3–4
$^{41-45}Ar(p,n)$	...	0.7–2.0	$\delta(A \geq 43)$	3–4
$^{43,45,47}Ar(\gamma,n)$	?	threshold	$\delta(A \geq 43)$	2
$^{39}K(n,\gamma)^{40}K$	7.80	≥ 0	$\delta(^{40}K)$	1
$^{40}K(n,\gamma)^{41}K$	10.09	≥ 0	$\delta(^{40}K)$	4
$^{40}K(n,p)^{40}Ar$	2.29	≥ 0	$\delta(^{40}K,^{40}Ar)$	3
$^{40}K(n,\alpha)^{37}Cl$	3.88	0–0.4	$\delta(^{40}K)$	4
$^{41-47}K(n,\gamma)$	...	≥ 0	$\delta(A \geq 43)$	3–4
$^{42-47}K(p,n)$	?	0.7–2.0	$\delta(^{43,46}Ca,^{45}Sc)$	3–4
$^{40}Ca(n,\gamma)^{41}Ca$	8.36	≥ 0	$\delta(A \geq 43)$	2
$^{40}Ca(n,p)^{40}K$	−0.53	1.3–2.6	$\delta(A \geq 43)$	2
$^{41}Ca(n,\gamma)^{42}Ca$	11.47	≥ 0	$\delta(A \geq 43)$	1
$^{41}Ca(n,p)^{41}K$	1.20	0–0.9	$\delta(A \geq 43)$	1
$^{41}Ca(n,\alpha)^{38}Ar$	5.23	≥ 0	$\delta(A \geq 40)$	1
$^{42}Ca(n,\gamma)^{43}Ca$	7.93	≥ 0	$\delta(^{43}Ca)$	4
$^{43}Ca(n,\gamma)^{44}Ca$	11.14	≥ 0	$\delta(^{43}Ca)$	3
$^{44}Ca(n,\gamma)^{45}Ca$	7.42	≥ 0	$\delta(^{45}Sc)$	4
$^{45}Ca(n,\gamma)^{46}Ca$	10.40	≥ 0	$\delta(^{45}Sc,^{46}Ca)$	3
$^{45}Ca(p,\gamma)^{46}Sc$	8.24	0.8–2.1	$\delta(^{47,49,50}Ti)$	4
$^{45}Ca(p,n)^{45}Sc$	−0.53	0.8–2.1	$\delta(^{45}Sc)$	3
$^{46}Ca(n,\gamma)^{47}Ca$	7.28	≥ 0	$\delta(^{46}Ca,^{47}Ti)$	3
$^{46}Ca(p,n)^{46}Sc$	−2.17	threshold	$\delta(^{46}Ca)$	3
$^{46}Ca(p,\gamma)^{47}Sc$	8.48	0.8–2.1	$\delta(^{46}Ca,^{47}Ti)$	4
$^{47}Ca(n,\gamma)^{48}Ca$	9.94	≥ 0	$\delta(^{47}Ti,^{48}Ca)$	3
$^{47}Ca(p,n)^{47}Sc$	1.20	0.8–2.1	$\delta(^{47}Ti)$	3
$^{47}Ca(p,\gamma)^{48}Sc$	9.45	0.8–2.1	$\delta(^{47}Ti)$	4
$^{48}Ca(n,\gamma)^{49}Ca$	5.14	≥ 0	$\delta(A \geq 48)$	3
$^{48}Ca(p,n)^{48}Sc$	−0.49	0.8–2.1	$\delta(A \geq 48)$	3
$^{48}Ca(p,\gamma)^{49}Sc$	9.62	0.8–2.1	$\delta(A \geq 48)$	2
$^{45-49}Sc(n,\gamma)$	...	≥ 0	$\delta(A \geq 48)$	3–4
$^{47-50}Sc(p,n)$	?	0.8–2.2	$\delta(^{47,49,50}Ti)$	3–4
$^{49}Sc(p,\gamma)^{50}Ti$	12.17	0.8–2.2	$\delta(^{50}Ti)$	4
$^{48}Ti(n,\gamma)^{49}Ti$	8.15	≥ 0	$\delta(^{49}Ti)$	4
$^{49}Ti(n,\gamma)^{50}Ti$	10.94	≥ 0	$\delta(^{49,50}Ti)$	3
$^{49}Ti(p,n)^{49}V$	−1.39	1.4–2.3	$\delta(^{49}Ti,^{50}V)$	3
$^{49}Ti(p,\gamma)^{50}V$	7.95	0.9–2.3	$\delta(^{49}Ti,^{50}V)$	3
$^{50}Ti(n,\gamma)^{51}Ti$	6.38	≥ 0	$\delta(^{50}Ti)$	3
$^{50}Ti(p,n)^{50}V$	−3.00	threshold	$\delta(^{50}Ti,^{50}V)$	3
$^{50}Ti(p,\gamma)^{51}V$	8.06	0.9–2.3	$\delta(^{50}Ti)$	4
$^{51}Ti(p,n)^{51}V$	1.68	0.9–2.3	$\delta(^{50}V)$	4
$^{49}V(n,\gamma)^{50}V$	9.34	≥ 0	$\delta(^{50}V)$	4
$^{50}V(n,\gamma)^{51}V$	11.05	≥ 0	$\delta(^{50}V)$	4
$^{61}Fe(\gamma,n)^{60}Fe$	−5.69	threshold	$\delta(^{60}Ni)$	1
$^{63}Fe(\gamma,n)^{62}Fe$	?	threshold	$\delta(^{62}Ni)$	1
$^{65}Fe(\gamma,n)^{64}Fe$	?	threshold	$\delta(^{64}Ni)$	1
$^{62}Fe(p,n)^{62}Co$	...	1.0–2.5	$\delta(^{65}Cu,^{67}Zn)$	1
$^{64}Fe(p,n)^{64}Co$	...	1.0–2.5	$\delta(^{65}Cu,^{67}Zn)$	1
$^{64}Co(\gamma,n)^{63}Co$	?	threshold	$\delta(^{65}Cu,^{67}Zn)$	3
$^{66}Co(\gamma,n)^{65}Co$	?	threshold	$\delta(^{65}Cu)$	2
$^{68}Co(\gamma,n)^{67}Co$	?	threshold	$\delta(^{67}Zn)$	2
$^{65}Co(p,n)^{65}Ni$	...	1.0–2.5	$\delta(^{65}Cu)$	1
$^{67}Co(p,n)^{67}Ni$	...	1.0–2.5	$\delta(^{67}Zn)$	1
$^{67}Ni(\gamma,n)^{66}Ni$	?	threshold	$\delta(^{68,70}An)$	2
$^{69}Ni(\gamma,n)^{68}Ni$	?	threshold	$\delta(^{68}Zn)$	1
$^{71}Ni(\gamma,n)^{70}Ni$	?	threshold	$\delta(^{70}Zn)$	2
$^{68}Ni(p,n)^{68}Cu$	...	1.1–2.6	$\delta(^{71}Ga,^{73}Ge)$	1
$^{70}Ni(p,n)^{70}Cu$	...	1.1–2.6	$\delta(^{71}Ga,^{73}Ge)$	1
$^{70}Cu(\gamma,n)^{69}Cu$	?	threshold	$\delta(^{71}Ga,^{73}Ge)$	3
$^{72}Cu(\gamma,n)^{71}Cu$	?	threshold	$\delta(^{71}Ga)$	2
$^{74}Cu(\gamma,n)^{73}Cu$	?	threshold	$\delta(^{73}Ge)$	2
$^{71}Cu(p,n)^{71}Zn$	...	1.1–2.6	$\delta(^{71}Ga)$	2
$^{73}Cu(p,n)^{73}Zn$	...	1.1–2.6	$\delta(^{73}Ge)$	2
$^{75}Zn(\gamma,n)^{74}Zn$	?	threshold	$\delta(^{76}Se)$	2
$^{77}Zn(\gamma,n)^{76}Zn$	?	threshold	$\delta(^{76}Se)$	2

E. Nucleosynthesis of rare nuclei from seed nuclei during explosive carbon burning

While the carbon fuses explosively in zone III into its primary products, an intense bath of free neutrons and protons pervades the gas. These free nucleons will interact with heavy nuclei that were present in small amounts from the beginning. These seed nuclei, of which $^{28,29,30}Si$, ^{31}P, $^{32,34}S$, $^{36,38}Ar$, ^{40}Ca, ^{52}Cr, $^{56,57}Fe$, and $^{58,60}Ni$ have initial mass fractions $X > 10^{-5}$ gm/gm, are thereby converted in part to rare nuclei having mass fractions in the range $10^{-8} < X < 10^{-7}$. These seed reactions have been shown (Howard *et al.*, 1972) to be a possible natural source of the rare nuclei ^{36}S, ^{40}Ar, ^{40}K, $^{43,46,48}Ca$, ^{45}Sc, $^{47,49,50}Ti$, ^{50}V, $^{63,65}Cu$, $^{62,64}Ni$, $^{68,70}Zn$, $^{69,71}Ga$, ^{73}Ge, ^{75}As, and ^{76}Ge. In almost all casses these nuclei appear to be bypassed by the primary modes of nucleosynthesis. Two examples will illustrate the character of this nucleosynthesis.

(a) The rare sulfur isotope ^{36}S is produced from seed $^{32,34}S$ and ^{36}Ar primarily by the following reaction sequences:

$$^{32}S(n,\gamma)^{33}S(n,\gamma)^{34}S(n,\gamma)^{35}S(n,\gamma)^{36}S$$

or

$$^{35}S(p,n)^{35}Cl(n,\gamma)^{36}Cl(n,p)^{36}S,$$

and

$$^{36}Ar(n,p)^{36}Cl(n,p)^{36}S.$$

TABLE IV. Reactions of importance during hydrostatic oxygen burning ($1.5 < T_9 < 2.5$), explosive oxygen burning ($3.0 < T_9 < 4.0$), and explosive silicon burning ($3.5 < T_9 < 5.5$).

Reaction	Q (MeV)	Energy Range (MeV)	Importance HyOx	Importance ExOx	Importance ExSi	Value HyOx	Value ExOx	Value ExSi
$^{12}C(\gamma,\alpha)^{8}Be$	−7.37	8.1–10.6		MBR	MBR		2	2
$^{12}C + ^{12}C$	α,p,n	3.7–9.7		MBR	MBR		1	2
$^{12}C + ^{16}O$	α,p,n,	4.9–12.0		MBR	MBR		1	2
$^{16}O + ^{16}O$	α,p,n,d	4.2–14.9	MBR	MBR	MBR	1	1	2
$^{16}O(\gamma,p)^{15}N$	−12.13	12.5–13.9		MBR			2	
$^{16}O(p,\alpha)^{13}N$	−5.22	6.5–9.9		MBR	MBR		1	1
$^{16}O(n,\alpha)^{13}C$	−2.21	3.3–6.5		MBR	MBR		1	2
$^{16}O(\gamma,\alpha)^{12}C$	−7.16	8.3–11.4		MBR	MBR		1	1
$^{20}Ne(\gamma,\alpha)^{16}O$	−4.73	6.2–9.8		MBR	MBR		2	2
$^{20}Ne(p,\alpha)^{17}F$	−4.13	5.9–9.6			MBR			2
$^{20}Ne(n,\alpha)^{17}O$	−0.59	2.2–5.7			MBR			3
$^{20}Ne(\alpha,\gamma)^{24}Mg$	−4.73	1.8–4.6		MBR			2	
$^{23}Na(p,\alpha)^{20}Ne$	2.38	0.6–4.3		MBR	MBR		2	3
$^{23}Na(p,\gamma)^{24}Mg$	11.69	0.6–2.3		MBR			2	
$^{23}Mg(n,p)^{23}Na$	4.84	≥ 0		MBR			4	
$^{24}Mg(\alpha,p)^{27}Al$	−1.60	2.1–6.5	$\delta(^{28}Si)$	MBR	↓MBR	3	2	3
$^{24}Mg(\alpha,\gamma)^{28}Si$	9.98	1.4–6.5	$\delta(^{28}Si)$	MBR	↓MBR	3	2	2
$^{24}Mg(p,\alpha)^{21}Na$	−6.88	9.0–13.0			MBR			1
$^{24}Mg(n,\alpha)^{21}Ne$	−2.56	4.5–8.4			MBR			1
$^{24}Mg(\gamma,\alpha)^{20}Ne$	−9.32	11.1–15.1		↓MBR	MBR		2	1
$^{26}Mg(p,\gamma)^{27}Al$	8.27	0.4–2.5	$\delta(\eta)$	MBR		4	4	
$^{26}Mg(\alpha,n)^{29}Si$	0.03	1.4–5.2	$\delta(^{29}Si)$	MBR		4	4	
$^{27}Al(n,\gamma)^{28}Al$	7.73	≥ 0	$\delta(\eta)$			2		
$^{27}Al(p,\gamma)^{28}Si$	11.58	0.5–3.2	$\delta(\eta)$	MBR	↓MBR	3	3	2
$^{27}Al(\alpha,p)^{30}S$	2.38	1.5–6.8	$\delta(\eta)$		$\delta(^{30}Si)$	3		4
$^{27}Al(p,n)^{27}Si$	−5.59	threshold		MBR			4	
$^{28}Al(p,n)^{28}Si$	3.85	0.5–1.8	$\delta(\eta)$			3		
$^{28}Si(n,\gamma)^{29}Si$	8.48	≥ 0	$\delta(^{29}Si)$	$\delta(^{29}Si)$	$\delta(^{29}Si)$	4	4	4
$^{28}Si(\alpha,p)^{31}P$	−1.92	2.5–7.2	$\delta(^{31}P)$	$\delta(^{31}P)$	$\delta(^{31}P)$	3	2	3
$^{28}Si(\alpha,\gamma)^{32}S$	6.95	1.6–7.2	$\delta(^{28}Si^{32}S)$	$\delta(^{28}Si^{32}S)$	$\delta(^{28}Si^{32}S)$	3	3	3
$^{29}Si(n,\gamma)^{30}Si$	10.62	≥ 0	$\delta(^{29}Si^{30}Si)$	$\delta(^{29}Si^{30}Si)$		4	4	
$^{29}Si(\alpha,n)^{32}S$	−1.53	1.6–7.2	$\delta(\eta)$	$\delta(^{29}Si)$	$\delta(^{29}Si)$	2	4	4
$^{30}Si(p,\gamma)^{31}P$	7.29	0.5–3.4	$\delta(^{30}Si^{31}P)$	$\delta(^{30}Si^{31}P)$	↓$\delta(^{31}P)$	3	4	4
$^{30}Si(\alpha,\gamma)^{34}S$	7.92	1.6–4.1	$\delta(^{30}Si^{34}S)$			4		
$^{30}Si(\alpha,n)^{33}S$	−3.50	3.5–7.2	↓$\delta(\eta)$	$\delta(^{30}Si^{33}S)$	$\delta(^{30}Si^{33}S)$	1	4	4
$^{30}Si(p,n,)^{30}P$	−5.03	threshold			$\delta(^{30}Si)$			4
$^{30}P(\gamma,p)^{29}Si$	−5.59	6.1–9.0	$\delta(\eta)$		$\delta(^{29}Si)$	2		4
$^{30}P(n,\alpha)^{27}Al$	2.65	0–4.2			$\delta(^{29}Si^{30}Si)$			4
$^{31}P(n,\gamma)^{32}P$	7.94	≥ 0	$\delta(^{31}P)$			4		
$^{31}P(p,\gamma)^{32}S$	8.86	0.6–3.5	$\delta(^{31}P)$	$\delta(^{31}P)$	$\delta(^{31}P)$	3	2	3
$^{31}P(\alpha,p)^{34}S$	0.63	1.7–6.0	$\delta(^{31}P^{34}S)$	$\delta(^{31}P^{34}S)$		4	4	
$^{32}P(p,n)^{32}S$	0.93	0.6–2.0	$\delta(^{32}S)$			4		
$^{33}P(p,n)^{33}S$	−0.53	0.6–2.0	$\delta(\eta)$			1		
$^{31}S(\gamma,p)^{30}P$	−6.08	6.6–8.1	$\delta(\eta)$			2		
$^{32}S(n,\gamma)^{33}S$	8.64	≥ 0	$\delta(\eta)$	$\delta(^{33}S)$	$\delta(^{33}S)$	1	3	4
$^{32}S(\alpha,p)^{35}Cl$	−1.86	2.5–7.8	$\delta(\eta)$	$\delta(^{35}Cl)$	↓$\delta(^{35}Cl)$	3	3	3
$^{32}S(\alpha,\gamma)^{36}Ar$	6.64	2.7–7.8		$\delta(^{32}S^{36}Ar)$	$\delta(^{32}S^{36}Ar)$		3	4
$^{33}S(n,\gamma)^{34}S$	11.42	≥ 0	$\delta(\eta)$			2		
$^{33}S(\alpha,p)^{36}Cl$	−1.93	2.8–6.2		$\delta(^{33}S)$			4	
$^{33}S(\alpha,n)^{36}Ar$	−2.00	2.7–6.2		$\delta(^{33}S)$			4	
$^{33}S(p,\alpha)^{30}P$	−1.52	4.4–9.0			$\delta(^{33}S)$			4
$^{34}S(p,\gamma)^{35}Cl$	6.37	0.6–3.6	$\delta(^{34}S^{35}Cl)$	$\delta(^{34}S^{35}Cl)$	$\delta(^{34}S^{35}Cl)$	3	3	4
$^{34}S(\alpha,\gamma)^{38}Ar$	7.21	1.8–6.2	$\delta(^{34}S^{38}Ar)$	$\delta(^{34}S^{38}Ar)$		4	3	
$^{34}S(\alpha,p)^{37}Cl$	−3.03	3.9–6.2		$\delta(^{34}S)$			3	
$^{34}S(\alpha,n)^{37}Ar$	−4.63	4.6–6.2		$\delta(^{34}S^{37}Cl)$			4	
$^{35}Cl(p,\gamma)^{36}Ar$	8.51	0.6–3.8	$\delta(^{35}Cl)$	$\delta(^{35}Cl)$	$\delta(^{35}Cl)$	3	3	3
$^{35}Cl(\alpha,p)^{38}Ar$	0.84	2.9–8.1		$\delta(^{35}Cl^{38}Ar)$	$\delta(^{35}Cl^{38}Ar)$		3	4
$^{37}Cl(p,\gamma)^{38}Ar$	10.24	0.9–3.0		$\delta(^{38}Ar)$			3	
$^{36}Ar(n,\gamma)^{37}Ar$	8.79	≥ 0		$\delta(^{37}Cl)$	$\delta(^{37}Cl)$		4	4
$^{36}Ar(\alpha,p)^{39}K$	−1.29	3.0–8.4		$\delta(^{39}K)$	↓$\delta(^{39}K)$		3	3
$^{36}Ar(\alpha,\gamma)^{40}Ca$	7.04	3.0–8.4		$\delta(^{36}Ar^{40}Ca)$	$\delta(^{36}Ar^{40}Ca)$		4	3
$^{37}Ar(n,p)^{37}Cl$	1.60	0–1.4		$\delta(^{37}Cl)$			4	
$^{37}Ar(\alpha,n)^{40}Ca$	−1.75	3.0–6.7		$\delta(^{37}Cl)$			4	
$^{38}Ar(p,\gamma)^{39}K$	6.37	1.0–3.9		$\delta(^{38}Ar^{39}K)$	$\delta(^{38}Ar^{39}K)$		3	4
$^{38}Ar(\alpha,n)^{41}Ca$	−5.23	5.2–6.7		$\delta(^{38}Ar^{41}K)$			4	
$^{38}Ar(\alpha,\gamma)^{42}Ca$	6.25	3.0–6.7		$\delta(^{38}Ar^{42}Ca)$			4	
$^{39}K(p,\gamma)^{40}Ca$	8.33	1.0–4.0		$\delta(^{39}K)$	$\delta(^{39}K)$		3	3
$^{39}K(\alpha,p)^{42}Ca$	−0.13	3.2–6.9		$\delta(^{39}K^{42}Ca)$			4	
$^{40}Ca(n,\gamma)^{41}Ca$	8.36	≥ 0		$\delta(^{41}K)$	$\delta(^{41}K)$		4	4
$^{40}Ca(\alpha,p)^{43}Sc$	−3.54	4.6–8.9		$\delta(^{46}Ti)$	$\delta(^{44}Ca)$,qe		3	4
$^{40}Ca(\alpha,\gamma)^{44}Ti$	5.24	3.3–8.9		$\delta(^{46}Ti)$	$\delta(^{44}Ca)$,qe		4	4

TABLE IV. (Continued).

Reaction	Q (MeV)	Energy Range (MeV)	Importance			Value		
			HyOx	ExOx	ExSi	HyOx	ExOx	ExSi
$^{41}Ca(\alpha,\gamma)^{45}Ti$	6.29	3.3–8.9		$\delta(^{46}Ti)$	$\delta(^{45}Sc)$,qe		4	4
$^{42}Ca(p,\gamma)^{43}Sc$	4.92	1.0–4.1		$\delta(^{46}Ti)$	$\delta(^{44}Ca)$,qe		4	4
$^{42}Ca(\alpha,p)^{45}Sc$	−2.34	3.4–8.9		$\delta(^{46}Ti)$	$\delta(^{45}Sc)$,qe		4	4
$^{42}Ca(\alpha,\gamma)^{46}Ti$	8.01	3.3–8.9		$\delta(^{46}Ti)$	qe		3	3
$^{45}Sc(p,\gamma)^{46}Ti$	10.35	1.1–4.2		$\delta(^{46}Ti)$	qe		2	2
$^{44}Ti(n,\gamma)^{45}Ti$	9.42	≥0		$\delta(^{46}Ti)$	$\delta(^{45}Sc)$,qe		4	3
$^{44}Ti(\alpha,p)^{47}V$	5.18	3.9–9.5			$\delta(^{47}Ti)$,qe			1
$^{45}Ti(n,\gamma)^{46}Ti$	13.19	≥0			qe			3
$^{45}Ti(n,p)^{45}Sc$	2.84	0–1.5		$\delta(^{46}Ti)$	qe		3	3
$^{46}Ti(n,\gamma)^{47}Ti$	8.88	≥0		$\delta(^{50}Cr)$			3	
$^{46}Ti(p,\gamma)^{47}V$	5.1–	1.1–4.3		$\delta(^{50}Cr)$	$\delta(^{46}Ti^{47}Ti)$		3	3
$^{47}Ti(p,\gamma)^{48}V$	6.83	1.1–4.3		$\delta(^{50}Cr)$	$\delta(^{47}Ti)$		3	3
$^{47}Ti(p,n)^{47}V$	−3.70	3.7–4.3		$\downarrow\delta(^{50}Cr)$	$\delta(^{47}Ti)$		3	3
$^{47}V(p,\gamma)^{48}Cr$	8.09	1.2–4.4		$\delta(^{50}Cr)$	$\delta(^{48}Ti)$		3	4
$^{48}V(p,\gamma)^{48}Cr$	8.21	1.2–4.4		$\delta(^{50}Cr)$	$\delta(^{49}Ti)$		3	3
$^{49}V(p,\gamma)^{50}Cr$	9.59	1.2–4.4		$\delta(^{50}Cr)$	$\delta(^{50}Cr)$		3	3
$^{48}Cr(n,p)^{48}V$	2.44	0–2.0		$\delta(^{50}Cr)$	$\delta(^{48}Ti)$		4	3
$^{49}Cr(n,p)^{49}V$	3.34	0–1.1		$\delta(^{50}Cr)$	$\delta(^{49}Ti)$		3	3
$^{50}Cr(n,\gamma)^{51}Cr$	9.27	≥0		$\delta(^{54}Fe)$	$\delta(^{50}Cr)$		3	4
$^{50}Cr(p,\gamma)^{51}Mn$	5.30	1.2–4.6		$\delta(^{54}Fe)$	$\delta(^{50}Sc^{51}V)$		4	3
$^{51}Cr(n,\gamma)^{52}Cr$	12.04	≥0		$\delta(^{54}Fe)$	$\delta(^{51}V)$		3	4
$^{51}Cr(p,\gamma)^{52}Mn$	6.54	1.2–4.6		$\delta(^{54}Fe)$	$\delta(^{51}V)$		3	4
$^{52}Cr(p,\gamma)^{53}Mn$	6.56	1.2–4.6		$\delta(^{54}Fe)$	$\delta(^{52}Cr^{54}Fe)$		3	4
$^{51}Mn(n,p)^{51}Cr$	3.97	0–0.6		$\delta(^{54}Fe)$	$\delta(^{51}V)$		3	4
$^{51}Mn(p,\gamma)^{52}Fe$	7.36	1.4–4.7			$\delta(^{51}V)$			3
$^{52}Mn(n,p)^{52}Cr$	5.49	≥0		$\delta(^{54}Fe)$	$\delta(^{52}Cr)$		4	4
$^{52}Mn(p,\gamma)^{53}Fe$	7.29	1.3–4.7		$\delta(^{54}Fe)$	$\delta(^{53}Cr)$		3	3
$^{53}Mn(p,\gamma)^{54}Fe$	8.85	1.3–4.7		$\delta(^{54}Fe)$	$\delta(^{53}Cr^{54}Fe)$		3	3
$^{52}Fe(n,\gamma)^{53}Fe$	10.44	≥0			$\delta(^{52}Cr^{53}Cr)$			4
$^{52}Fe(n,p)^{52}Mn$	3.16	0–1.5			$\delta(^{52}Cr)$			4
$^{53}Fe(n,p)^{53}Mn$	4.77	≥0		$\delta(^{54}Fe)$	$\delta(^{53}Cr)$		3	3
$^{54}Fe(n,\gamma)^{55}Fe$	9.30	≥0			$\delta(^{55}Mn)$			4
$^{54}Fe(p,\gamma)^{55}Co$	5.06	1.5–4.8			$\delta(^{55}Mn)$			3
$^{54}Fe(\alpha,p)^{57}Co$	−1.77	4.5–10.5			$\delta(^{54}Fe^{58}Ni)$			3
$^{55}Fe(p,n)^{55}Co$	−4.24	4.2–4.8			$\delta(^{55}Mn)$			4
$^{55}Fe(p,\gamma)^{56}Co$	5.85	1.5–4.8			$\delta(^{55}Mn^{57}Fe)$			3
$^{55}Co(p,\gamma)^{56}Ni$	7.17	1.5–4.9			$\delta(^{55}Mn)$			3
$^{56}Co(p,\gamma)^{57}Ni$	7.36	1.5–4.9			$\delta(^{57}Fe)$			3
$^{57}Co(p,\gamma)^{58}Ni$	8.18	1.5–4.9			$\delta(^{58}Ni)$			3
$^{56}Ni(n,\gamma)^{57}Ni$	10.28	≥0			$\delta(^{57}Fe)$			3
$^{56}Ni(n,p)^{56}Co$	2.91	0–2.0			$\delta(^{56}Fe)$			3
$^{57}Ni(n,p)^{57}Co$	4.02	0–0.9			$\delta(^{57}Fe^{58}Ni)$			3
$^{58}Ni(p,\gamma)^{59}Cu$	3.42	1.6–5.0			$\delta(^{58}Ni^{59}Cu)$			3
$^{59}Cu(p,\gamma)^{60}Zn$	5.12	1.6–5.1			$\delta(^{59}Co^{60}Zn)$			3
$^{59}Cu(p,\alpha)^{56}Ni$	2.40	2.4–8.6			$\delta(^{59}Co^{56}Fe)$			3
$^{60}Cu(p,\gamma)^{61}Zn$	5.52	1.6–5.1			$\delta(^{61}Ni)$			3
$^{60}Cu(p,\alpha)^{57}Ni$	2.62	2.1–8.4			$\delta(^{57}Fe)$			3

These reactions and several others are important in determining the rate of production of ^{36}S. Some of the important reaction currents are shown in Fig. 8. During the early neutron-dominated phase, which results from rapid release of neutrons when the carbon ignition begins, the ^{36}S is built to a large abundance through the above reactions. After the initial burst of neutrons has been captured, the gas is proton dominated until it cools. During this period the ^{36}S abundance is greatly reduced by the $^{36}S(p,\gamma)^{37}Cl$ reaction, whose cross section is one of the most important for nuclear astrophysics. Measurement of the key reaction rates will indicate the neutron and proton densities nature has used during the explosive expansions. See Howard *et al.*, (1972) for many details.

(b) The rare nickel isotopes $^{62,64}Ni$ are synthesized primarily by neutron-capture chains originating from ^{56}Fe seed nuclei. The (n,γ) cross sections are large enough that during the neutron-dominated phase the iron seed is quickly driven out to more massive isotopes until it is stopped by (γ,n) reactions on an isotope having a low (~4.5–5.0MeV) neutron separation energy. Several neutron separation energies need be determined before definitive quantitative analysis can be made. The situation resembles the traditional *r* process (Clayton, 1968), but it is not so discouragingly far into the neutron-rich region. The photoneutron reactions seem to naturally occur at ^{63}Fe and ^{65}Fe, thereby stopping the flow at ^{62}Fe and ^{64}Fe, which in turn decay to ^{62}Ni and ^{64}Ni after the explosion. The yields of odd-A nuclei are very temperature sensitive because they depend on (p,n) reaction rates on isotopes of Fe and Ni.

Table III lists the seed reactions of importance during the explosive burning of carbon. Unknown but interesting

neutron separation energies are indicated by question marks in the Q column. In this whole system there exist great challenges for laboratory nuclear astrophysics.

F. Hydrostatic oxygen burning in stars

The fusion of oxygen in stars in a state of hydrostatic equilibrium occurs in the temperature range $1.5 < T_9 < 2.5$. It has a twofold importance: (1) the thermonuclear power can balance the energy loss due to neutrinos for a few weeks to a few years, thereby providing a short but significant epoch in the preterminal stages of the star's life; (2) the thermonuclear products cannot escape from the star, but they do provide the initial composition for an explosive ejection late in oxygen burning or during silicon burning. Insofar as thermonuclear power is concerned, almost the only cross section of great importance is that for the reaction of ^{16}O with itself. However, many cross sections are important for determining the evolution of the composition. The most important are those which control the production of e^+-emitting or e^--capturing nuclei, because they control the degree of neutron enrichment that may occur. The number of excess neutrons per nucleon, η, has a strong influence on the nuclear composition that can leave the star later. The reactions important in this regard are designated by $\delta(\eta)$ in Table IV. For example, weakly decaying ^{31}S is produced primarily by ^{16}O(^{16}O,n)^{31}S and destroyed by its decays, (e^+,ν) and (e^-,ν) and by ^{31}S$(\gamma,p)^{30}$P. The latter reaction therefore ranks value 2 in Table IV, but the cross section may be unmeasurable since the targets are not stable in either direction. The production of e^--capturing ^{33}S is also quite important. Its chief mode of destruction, ^{33}S$(n,\alpha)^{30}$Si rates a value 1 in Table IV (where it is listed under the reverse reaction). See Woosley, Arnett, and Clayton (1972a) for the nuclear details.

G. Explosive oxygen burning

The explosive ejection of ^{16}O-burning shells can easily synthesize the following set of nuclei in ratios agreeing well with the solar abundances: $\{X(E\,x\,O)\}$ = ^{28}Si, ^{32,33,34}S, ^{35,37}Cl, ^{36,38}Ar, ^{39,41}K, ^{40,42}Ca, ^{46}Ti, and ^{50}Cr. The excellent nature of this correspondence, shown in Fig. 9, reaffirms our belief that the natural abundances reflect nuclear properties, and it also argues even more convincingly than did the carbon burning shells that thermonuclear explosions of carbon and oxygen are common in nature. The nature of the burning process has been carefully studied by Woosley, Arnett, and Clayton (1973), and the important reactions are included in Table IV. The interesting nuclear events revolve around basically three subjects: (1) the various modes by which ^{16}O is burned and the densities of free protons, neutrons and alphas produced by the burning. Primary is the reaction of ^{16}O with itself, but also of importance are the reactions ^{16}O$(p,\alpha)^{13}$N discussed earlier, ^{16}O$(n,\alpha)^{13}$C, ^{16}O$(\gamma,p)^{15}$N, and ^{16}O$(\gamma,\alpha)^{12}$C and their sequels. These are called the "main burning reactions" and are designated by MBR in Table IV; (2) between ^{28}Si and ^{42}Ca the synthesized nuclei quickly form quasiequilibrium clusters (Woosley, Arnett, and Clayton, 1973; Bodansky, Clayton, and Fowler, 1968) with respect to exchange of protons, neutrons, alphas, and photons. These clusters merge until there is a single cluster in this mass range before

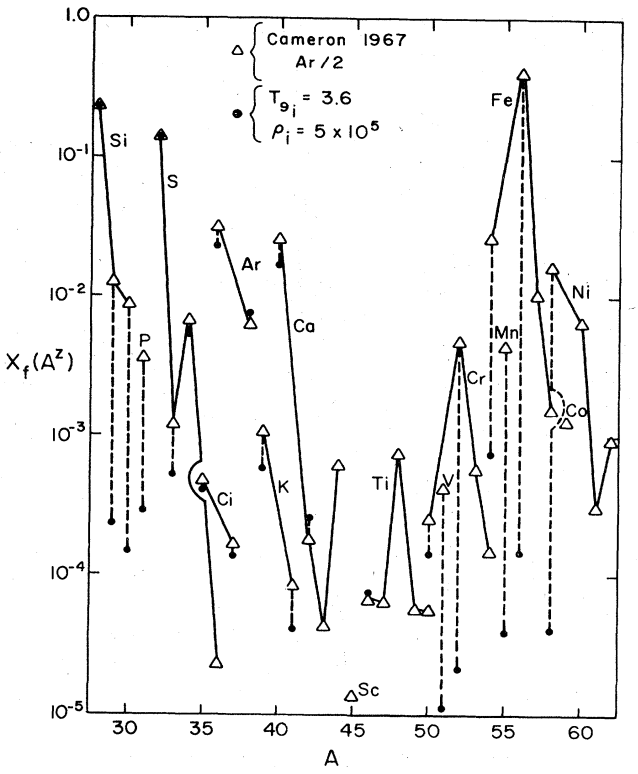

FIG. 9. The calculated products of explosive oxygen burning, shown as solid dots, are compared (Woosley, Arnett, Clayton, 1973) with the natural abundances, shown as open triangles. The impressive agreement between $A = 28$ and $A = 42$ except for ^{29,30}Si, ^{31}P, and ^{36}S, which are synthesized in exploding carbon shells, argues strongly that these nuclei owe their existence to natural themonuclear explosions of oxygen.

the oxygen is depleted. Although the abundances do not at this stage depend directly upon the values of the cross sections participating in the quasiequilibrium, many reactions reassert their influence as the material cools in its expansion. For example, Table IV shows that the reaction ^{39}K$(p,\gamma)^{40}$Ca plays a significant role in determining the final overabundance $\delta(^{39}\text{K})$ that survives the cooling; (3) the cluster $28 \leq A \leq 42$ penetrates through an abundance minimum near $A = 44$, thereby transferring nuclei into the iron peak. A complicated set of reactions, the most important being ^{45}Sc$(p,\gamma)^{46}$Ti, feeds this transfer through the nuclei ^{46}Ti, ^{50}Cr, and ^{54}Fe. By the time a significant abundance of ^{54}Fe is established, however, its excess neutrons have robbed the quasiequilibrium cluster below $A = 44$ of its excess neutrons, thereby sabotaging the synthesis of its neutron-rich members. Either the majority of oxygen burning circumstances have not built large ^{54}Fe abundances or the burning has continued to the point where most of the nuclei have penetrated through to the iron peak.

Woosley, Arnett, and Clayton (1973) have studied the astrophysical conditions (density, peak temperature, expansion time) that yield the observed abundances, and their paper is a thorough guide to the problem. This phase of explosive burning is one of the richest for astrophysical constraints, nucleosynthesis detail, and for nuclear physics applications.

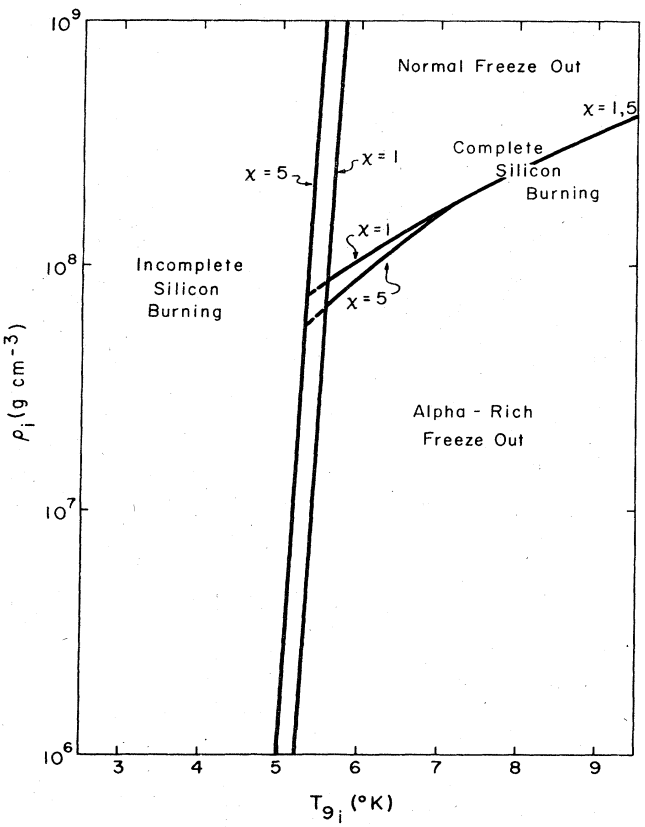

FIG. 10. Final state of explosions from differing initial temperatures (T_{9i}) and densities (ρ_i). For $T_{9i} < 5$, ^{28}Si is not completely burned and quasiequilibrium with ^{28}Si exists in the ejecta. For $T_{9i} > 5.5$, nuclear equilibrium is established and has a normal freeze-out at high initial density; however, for $\rho_i < 10^8$ gm cm^{-3}, excess free particles remain as the nuclear equilibrium expands and cools. Final abundances differ markedly for ejecta from these three differing types of explosions (Woosley, Arnett, and Clayton, 1973). The use of two time-scale parameters χ shows that the expansion rate has only a weak influence on this result.

H. Silicon burning

When oxygen has been exhausted, the next nucleus regulating further abundance change is ^{28}Si. Its photodisintegration and associated rearrangement into more massive nuclei is called silicon burning (Bodansky, Clayton, and Fowler, 1968). In stellar cores it occurs quickly because the energy release is less than in oxygen burning, which lasts no more than a year or so itself, whereas the higher temperature produces very much greater neutrino losses; actually, it cannot qualify for a hydrostatic burning phase because the star must adjust too quickly. In any case material in core silicon burning is not expected to ever get out of the star except, possibly, as matter that has first achieved nuclear statistical equilibrium. Therefore, the nuclear details of hydrostatic silicon burning are not of obviously high interest.

Silicon burning in explosively ejected debris, on the other hand, seem more likely to occur in presupernova oxygen zones (zones IV) that are explosively heated to such high temperatures that the oxygen has quickly burned. In that case, the nuclear evolution is being controlled by ^{28}Si. The reactions designated *qe* in Table IV are the ones controlling the merging of the quasiequilibrium for $28 \leq A \leq 44$ into full ^{28}Si based quasiequilibrium (Bodansky, Clayton, and Fowler, 1968) encompassing $28 \leq A \leq 58$. Most of the nuclear reactions other than the main burning reactions are only of modest importance during the explosive silicon burning, earning values of 3 or 4 on our scale in Table IV. Their importance, as noted there, is for the most part in determining the change δ of some abundance during the freezing of the nuclear distribution. Once again the reader should look for details at the paper of Woosley, Arnett, and Clayton (1973).

It is not clear that nature ejects partially burned silicon at all. Woosley, Arnett, and Clayton (1973) have shown that expansions of oxygen burning debris accompanied by hotter matter in nuclear statistical equilibrium (*e* process) gives an adequate account of observed abundances. The corresponding astrophysical possibility would be that whenever the temperature was high enough to consume the oxygen, it is also usually high enough to "melt" all the ^{28}Si and produce an *e* process. The last dozen or so reactions in Table IV are primarily those participating in the *e* process freeze-out. It is of considerable interest, especially for gamma-ray astronomy (Clayton, 1973), that the satisfactory *e* process must have a small neutron enrichment (Haineback *et al.*, 1974), say $\eta \approx 0.002$ neutrons per nucleon. It then follows that ^{56}Fe and ^{57}Fe were ejected as radioactive progenitors ^{56}Ni and ^{57}Ni, giving rise to an astronomical test with the radioactivity gamma rays. Haineback *et al.* (1974) discuss these nuclear points thoroughly. The set of *e*-process nuclei of low η is $\{X(e)\} =$ ^{48,49}Ti, ^{50,52,43}Cr, ^{51}V, ^{55}Mn, ^{54,56,57}Fe, and ^{58}Ni. These are the ones synthesized if ^{28}Si is completely exhausted in the explosive burning and if the free particles are recaptured during the cooling.

I. Particle-rich *e* process

If the peak temperature is as high as $T_9 = 5.5$, matter will achieve the state of statistical equilibrium (Woosley, Arnett, and Clayton, 1973). In high-temperature cases the bulk of the matter may be in the free alpha particles and nucleons, with only a small mass fraction in the iron peak nuclei. As the matter expands and cools, it "wants statistically" to recombine into the favored iron peak nuclei, but that is not always possible due to the intrinsically slow rate with which alpha particles can reassemble into heavier nuclei via the 3α reaction. Under these circumstances the material can cool to iron peak nuclei in an "excess" bath of alpha particles and nucleons. Woosley, Arnett, and Clayton (1973) have called this a particle-rich freeze-out because the free-particle number density is much greater than it would be at the same temperature in full equilibrium. A quasiequilibrium will exist, however, in which nuclei more massive than $A = 56$ will be greatly enhanced in abundance. For example, although $A = 60$ has low abundance in true equilibrium, it has a quite substantial final abundance in the particle-rich freeze-out due to, for example, ^{56}Ni$(\alpha,\gamma)^{60}$Zn. Figure 10 shows the peak conditions of the explosions of oxygen and silicon that lead to various descriptions of the expanding debris. The alpha-rich freeze-out of a statistical equilibrium is seen to be characteristic of the highest temperatures and lowest densities. The system of freeze-out reactions listed in Table

TABLE V. Reactions of importance during particle-rich *e*-process and freeze-out ($2.0 \leq T_9 \leq 5.0$).

Reaction	Q (MeV)	Energy range (MeV)	Importance	Value
3α	7.37	0.6–3.1	MBR	1
^{44}Ti$(\alpha,p)^{47}$V	—0.51	2.8–8.8	$\delta(^{44}$Ca)	1
^{44}Ti$(\alpha,\gamma)^{48}$Cr	7.58	2.8–8.8	$\delta(^{44}$Ca)	2
^{56}Ni$(p,\gamma)^{57}$Cu	(0.7)	1.1–4.6	$\delta(^{60}$Ni)	3
^{56}Ni$(\alpha,p)^{59}$Cu	−2.40	3.6–10.3	$\delta(^{59}$Co)	1
^{56}Ni$(\alpha,\gamma)^{60}$Zn	2.71	3.4–10.3	$\delta(^{60}$Ni)	2
^{57}Ni$(p,\gamma)^{58}$Cu	2.84	1.1–4.6	$\delta(^{60}$Ni)	2
^{57}Ni$(\alpha,p)^{60}$Cu	−2.62	3.8–10.3	$\delta(^{61}$Ni)	2
^{57}Ni$(\alpha,\gamma)^{61}$Zn	2.90	3.4–10.3	$\delta(^{61}$Ni)	3
^{58}Ni$(p,\gamma)^{59}$Cu	3.42	1.1–4.6	$\delta(^{59}$Co)	1
^{58}Ni$(\alpha,p)^{61}$Cu	−3.11	4.3–10.3	$\delta(^{62}$Ni)	2
^{58}Ni$(\alpha,\gamma)^{62}$Zn	3.32	3.4–10.3	$\delta(^{62}$Ni)	3
^{57}Cu$(p,\gamma)^{58}$Zn	(2.3)	1.2–4.7	$\delta(^{59}$Co)	4
^{57}Cu$(\alpha,p)^{60}$Zn	(2.0)	3.5–10.5	$\delta(^{60}$Ni)	4
^{58}Cu$(p,\gamma)^{59}$Zn	(2.9)	1.2–4.7	$\delta(^{59}$Co)	3
^{58}Cu$(\alpha,p)^{61}$Zn	0.06	3.5–10.5	$\delta(^{61}$Ni)	3
^{59}Cu$(p,\gamma)^{60}$Zn	5.12	1.2–4.7	$\delta(^{60}$Ni)	1
^{59}Cu$(\alpha,p)^{62}$Zn	−0.10	3.5–10.5	$\delta(^{62}$Ni)	2
^{60}Cu$(p,\gamma)^{61}$Zn	5.52	1.2–4.7	$\delta(^{61}$Ni)	3
^{61}Cu$(p,\gamma)^{62}$Zn	6.43	1.2–4.7	$\delta(^{62}$Ni)	4
^{58}Zn$(\alpha,p)^{61}$Ga	(1.8)	3.6–10.7	$\delta(^{64}$Zn)	4
^{59}Zn$(\alpha,p)^{62}$Ga	(−1.0)	3.6–10.7	$\delta(^{64}$Zn)	3
^{60}Zn$(p,\gamma)^{61}$Ga	(2.1)	1.2–4.8	$\delta(^{64}$Zn)	4
^{60}Zn$(\alpha,p)^{63}$Ga	−2.33	3.6–10.7	$\delta(^{64}$Zn)	2
^{60}Zn$(\alpha,\gamma)^{64}$Ge	2.65	3.6–10.7	$\delta(^{64}$Zn)	3
^{61}Zn$(p,\gamma)^{62}$Ga	(1.7)	1.2–4.8	$\delta(^{65}$Cu)	3
^{61}Zn$(\alpha,p)^{64}$Ga	−2.52	3.8–10.7	$\delta(^{65}$Cu)	4
^{61}Zn$(\alpha,\gamma)^{65}$Ge	2.11	3.6–10.7	$\delta(^{65}$Cu)	4
^{62}Zn$(p,\gamma)^{63}$Ga	2.89	1.2–4.8	$\delta(^{64}$Zn)	3
^{62}Zn$(\alpha,p)^{65}$Ga	−3.33	4.6–10.7	$\delta(^{66}$Zn)	3
^{62}Zn$(\alpha,\gamma)^{66}$Ge	2.04	3.6–10.7	$\delta(^{66}$Zn)	3
^{61}Ga$(\alpha,p)^{64}$Ge	(0.6)	3.7–10.9	$\delta(^{64}$Zn)	4
^{62}Ga$(\alpha,p)^{65}$Ge	(0.4)	3.7–10.9	$\delta(^{65}$Cu)	4
^{63}Ga$(p,\gamma)^{64}$Ge	(5.0)	1.2–4.9	$\delta(^{64}$Zn)	2
^{63}Ga$(\alpha,p)^{66}$Ge	−0.84	3.7–10.9	$\delta(^{66}$Zn)	4
^{64}Ga$(p,\gamma)^{65}$Ge	4.62	1.2–4.9	$\delta(^{65}$Cu)	4
^{65}Ga$(p,\gamma)^{66}$Ge	5.37	1.2–4.9	$\delta(^{66}$Zn)	3
^{64}Ge$(\alpha,p)^{67}$As	(−3.2)	4.5–11.1	$\delta(^{67}$Zn)	3
^{64}Ge$(\alpha,\gamma)^{68}$Se	(1.6)	3.8–11.1	$\delta(^{68}$Zn)	3
^{65}Ge$(\alpha,p)^{68}$As	(−2.7)	4.0–1.11	$\delta(^{69}$Ga)	4
^{65}Ge$(\alpha,\gamma)^{69}$Se	(2.4)	3.8–11.1	$\delta(^{69}$Ga)	4
^{66}Ge$(p,\gamma)^{67}$As	(2.7)	1.3–5.0	$\delta(^{67}$Zn)	3
^{66}Ge$(\alpha,p)^{69}$As	−2.40	3.8–11.1	$\delta(^{70}$Ge)	3
^{66}Ge$(\alpha,\gamma)^{70}$Se	(3.3)	3.8–11.1	$\delta(^{70}$Ge)	3
^{67}As$(p,\gamma)^{68}$Se	(4.7)	1.3–5.1	$\delta(^{68}$Zn)	2
^{67}As$(\alpha,p)^{70}$Se	(0.6)	3.9–11.4	$\delta(^{70}$Ge)	4
^{68}As$(p,\gamma)^{69}$Se	(5.1)	1.3–5.1	$\delta(^{69}$Ga)	4
^{69}As$(p,\gamma)^{70}$Se	(5.7)	1.3–5.1	$\delta(^{70}$Ga)	3
^{68}Se$(\alpha,p)^{71}$Br	(−2.0)	3.9–11.6	$\delta(^{71}$Ga)	2
^{68}Se$(\alpha,\gamma)^{72}$Kr	(2.7)	3.9–11.6	$\delta(^{72}$Ge)	3
^{69}Se$(\alpha,p)^{72}$Br	(−2.2)	3.9–11.6	$\delta(^{73}$Ge)	4
^{69}Se$(\alpha,\gamma)^{73}$Kr	(2.8)	3.9–11.6	$\delta(^{73}$Ge)	4
^{70}Se$(p,\gamma)^{71}$Br	(2.2)	1.3–5.2	$\delta(^{71}$Ga)	3
^{70}Se$(\alpha,p)^{73}$Br	(−3.0)	4.4–11.6	$\delta(^{74}$Se)	3
^{70}Se$(\alpha,\gamma)^{74}$Kr	(3.2)	3.9–11.6	$\delta(^{74}$Se)	3
^{71}Br$(\alpha,p)^{74}$Kr	(1.0)	4.0–11.8	$\delta(^{74}$Se)	4
^{71}Br$(p,\gamma)^{72}$Kr	(4.7)	1.4–5.3	$\delta(^{72}$Ge)	2
^{72}Br$(p,\gamma)^{73}$Kr	(4.9)	1.4–5.3	$\delta(^{73}$Ge)	4
^{73}Br$(p,\gamma)^{74}$Kr	6.13	1.4–5.3	$\delta(^{74}$Ge)	3

V has many challenges for laboratory physics. They occur primarily on the proton-rich side of the valley of beta stability. Even many Q values are unknown (at least to us) and we include parentheses around those obtained from semiempirical estimates.

It is still too early to say exactly which nuclei owe their existence to the particle-rich freeze-out, because many that are produced with very promising yields in this way are also synthesizable in principle by other events, such as the seed reactions during explosive carbon burning (Howard *et al.*, 1972) or by the *s* process (Peters, Fowler, and Clayton, 1972). It is extremely important for astrophysics to determine the extent to which the particle-rich freeze-out has occured in nature, because its demands on the explosive conditions can reveal much about the nature of the explosions. For the same reason, knowledge of the charged-particle cross sections will help pin down the actual free-particle densities.

We must close out discussion of important reactions at this point. We certainly have not discussed all of thermonuclear astrophysics. In particular we have almost ignored the elements heavier than zinc. Our attention to explosive burning in the intermediate-mass range perhaps qualifies us for the subtitle "Handbuch über Explosives Brennen." We are grateful for the advice of Professor William A. Fowler during the writing of our papers reported here. Much of the work was done at the Institute of Theoretical Astronomy, Cambridge, where we received encouragement and generous allocations of computer time from Professor Sir Fred Hoyle. This research was supported by the National Science Foundation GP-18335.

REFERENCES

Allen, B. J., J. H. Gibbons, and R. L. Macklin, 1971, Adv. Nucl. Phys **4,** 205.

Arnett, W. D., 1969, Astrophys. J. **157,** 1369.

Arnett, W. D., and J. W. Truran, 1969, Astrophys. J. **157,** 339.

Barnes, C. A., 1971, Adv. Nucl. Phys. **4,** 133.

Bodansky, D., D. D. Clayton, and W. A. Fowler, 1968, Astrophys. J. Suppl. Ser. **16,** 229.

Burlidge, E. M., G. R. Burlidge, W. A. Fowler, and F. Hoyle, 1957, Rev. Mod. Phys. **29,** 547.

Cameron, A. G. W., and W. A. Fowler, 1971, Astrophys. J. **164,** 111.

Clayton, D. D., 1973, in *Explosive Nucleosynthesis,* edited by W. D. Arnett, and D. N. Schramm (Texas U.P., Austin, Texas, 1973).

Clayton, D. D., S. A. Colgate, and G. J. Fishman, 1969, Astrophys. J. **155,** 75.

Clayton, D. D., W. A. Fowler, T. E. Hull, and B. A. Zimmerman, 1961, Ann. Phys. (N.Y.) **12,** 331.

Clayton, D. D., and F. Hoyle, 1974, Astrophys. J. **187,** L101.

Fowler, W. A., G. R. Caughlan, and B. A. Zimmerman, 1967, Annu. Rev. Astron. Astrophys. **5,** 525; sequel in preparation for same journal.

Hainebach, K., W. D. Arnett, S. E. Woosley, and D. D. Clayton 1974, Astrophys. J. **193,** October 1.

Howard, W. M., W. D. Arnett, and D. D. Clayton, 1971, Astrophys. J. **165,** 495.

Howard, W. M., W. D. Arnett, D. D. Clayton, and S. E. Woosley, 1972, Astrophys. J. **175,** 201.

Lyons, P. B., J. W. Toevs, and D. G. Sargood, 1969, Nucl. Phys. A **130,** 1.

Macklin, R. L., and J. H. Gibbons, 1965, Rev. Mod. Phys. **37,** 166.

Michaud, G., and W. A. Fowler, 1970, Phys. Rev. C **2,** 2041.

New Uses for Low Energy Accelerators, ad hoc panel of the National Research Council, W. A. Fowler, chairman (National Academy of Science: Washington, D.C., 1968).

Peters, J. G., W. A. Fowler, and D. D. Clayton, 1972, Astrophys. J. **173,** 637.

Starrfield, S., J. W. Truran, W. M. Sparks, and G. S. Kutler, 1972, Astophys. J., **176,** 169.

Woosley, S. E., 1973, Astrophys. J. **186,** 601.

Woosley, S. E., W. D. Arnett, and D. D. Clayton, 1972a, Astrophys. J. **175,** 731.

Woosley, S. E., W. D. Arnett, and D. D. Clayton, 1972b, Phys. Lett. B **38,** 196.

Woosley, S. E., W. D. Arnett, and D. D. Clayton, 1973, Astrophys. J. Suppl. Ser. **26,** 231.